UNITED NATIONS EDUCATIONAL, SCIENTIFIC AND CULTURAL ORGANIZATION
INTERNATIONAL ATOMIC ENERGY AGENCY
INTERNATIONAL CENTRE FOR THEORETICAL PHYSICS
I.C.T.P., P.O. BOX 586, 34100 TRIESTE, ITALY, CABLE: CENTRATOM TRIESTE

SMR/930 - 18

"Workshop on El Niño, Southern Oscillation and Monsoon"
15 - 26 July 1996

"ENSO Cycle & Anomalies of Winter Monsoon in East Asia"

LI CHONGYIN
Institute of Atmospheric Physics
Beijing
China

Please note: These are preliminary notes intended for internal distribution only.

ENSO CYCLE AND ANOMALIES OF WINTER MONSOON IN EAST ASIA

Li Chongyin
LASG, Institute of Atmospheric Physics, Academia Sinica
Beijing 100080, China

Abstract

The interactions between anomalous winter monsoon in East Asia and ENSO are further studied in this paper. The new results still more proved previous conclusion: there are clear interactions between ENSO and winter monsoon in East Asia. The continual westerly burst and stronger cumulus convection over the equatorial western Pacific caused by stronger winter monsoon in East Asia can respectively excite anomalous oceanic Kelvin wave and stronger atmospheric intraseasonal oscillation in the tropics, then the El Nino event will be produced through air-sea interaction; In El Nino winter, there are warmer and weaker winter monsoon in East Asia, this shown an important effect of El Nino to winter monsoon in East Asia. For La Nina case, the evolution of winter monsoon in East Asia is contrary to that in El Nino case. The ENSO cycle and aomalous strong and weak East-Asian winter monsoon cycle show clear interaction.

I. Introduction

Based on the data diagnostic and theoretical analysis, we have indicated firstly in 1988 that the precedence sign of El Nino event is in the equatorial western Pacific area and the frequent actions of stronger East-Asian aero troughs (cold waves) in the wintertime play an important role in exciting El Nino event[1]. Then the analyses further shown that there are clear interactions between anomalous circulation/climate in East Asia, especially the East Asian monsoon and El Nino event[2]. The frequent and stronger cold waves (the continuous stronger winter monsoon) in East Asia should lead the trade wind to be weakened (anomalous westerly) and the cumulus convection to be enhanced over the equatorial western Pacific. The stronger 30-60 day oscillations caused by the stronger convection activities over the equatorial Pacific and the anomalous oceanic Kelvin waves caused by anomalous westerly will play an important role in the occurrence of El Nino event. Therefore, it can be suggested that the anomalous strong winter monsoon (prior to El Nino) in East Asia is an important mechanism to excite El Nino event. In El Nino winter, the sea surface temperature anomalies (SSTA) in the equatorial eastern Pacific will lead the

Hadley cell, Ferrel circulation and the westerlies in the middle latitudes to the enhancements; and the polar front to the north in East Asia. Thus the southward outbreak of cold waves is unfavourable in East Asia. Therefore, there are higher surface temperature and weaker winter monsoon in East Asia in El Nino winter.

Recent years, some studies have also touched upon the relationship between the Asian summer monsoon and ENSO[3,4]. But some relationships are contemporaneous and the monsoon anomalies usually result from El Nino event, such as the anomalies of monsoon rainfall in India are mainly caused by El Nino event. It is difficult to investigate the mechanism exciting El Nino event based on these relationship.

In this paper, the relationship between ENSO and anomalous winter monsoon in East Asia will be studied. The result show that there are clear interactions between ENSO cycle and anomalous (strong and weak) winter monsoon in East Asia. It will be favourable to expose the mechanism of ENSO.

II. Anomalies of Cold Wave in East Asia and ENSO

The outbreak of cold air (cold wave activity) associated with aerotrough in East Asia is very important large-scale atmospheric process in the Northern Hemisphere in wintertime. The activity of cold wave is direct cause to produce winter monsoon and its variation in East Asia. In general, if there are stronger (weaker) cold wave activities, the winter monsoon in East Asia is also stronger (weaker), and the intensity of cold wave can be represented by using the surface air temperature in East Asia and the surface pressure in Siberia area or the aerotrough over East Asia. The analyses have found that there are strong and frequent cold wave activities in East Asia prior to the occurrence of El Nino. The anomalies of cold waves in East Asia prior to El Nino events are shown in Table 1, positive anomalies of surface pressure in (105°-120°E, 40°-60°N) region and negative anomalies of surface air temperature in eastern China (averaged for 15 stations from Beijing to Guangzhou) identically illustrated frequent strong cold wave activities in East Asia prior to the occurrence of El Nino event. Oppositely, prior to the occurrence of La Nina, there are weak cold waves in East Asia in wintertime.

Table 1 The surface pressure anomalies (Δp_s) in the region (105°-120°E, 40°-60°N) and the temperature anomalies (ΔT_s) in Eastern China during wintertime (Nov.-Apr.) prior to El Nino events

	1950.11 / 1951.4	1952.11 / 1953.4	1956.11 / 1957.4	1962.11 / 1963.4	1964.11 / 1965.4	1967.11 / 1968.4	1971.11 / 1972.4	1975.11 / 1976.4	1981.11 / 1982.4	1985.11 / 1986.4
$\Delta p_s(hPa)$	4.3	12.0	21.4	2.3	-2.4	12.0	6.8	5.8	2.6	3.4
$\Delta T_s(^\circ C)$	-4.1	-1.2	-9.0	-0.3	1.5	-6.0	-2.5	-1.5	-0.7	-1.8

In order to illustrate the relationship between ENSO and anomalies of cold wave in East Asia, the time-longitudes sections of the height anomalies at 500hPa over (20°-45°N) latitudes for warm case (El Nino) and cold case (La Nina) in 1980's are shown in Fig.1, respectively. It is clear that there are negative height anomalies over East Asia (about 110°-160°E region), which show strong aerotrough (cold wave) activities during wintertime prior to El Nino; and positive height anomalies over East Asia, which show weak aerotrough (cold wave) activities during El Nino wintertime. But, there are positive height anomalies over East Asia during wintertime prior to La Nina; and negative height anomalies during La Nina wintertime.

Therefore, it is clearly shown based on the data analyses that the anomalies of cold wave in East Asia is closely related to ENSO; there are strong (weak) cold wave activities in East Asia during wintertime prior to El Nino (La Nina), but there are weak (strong) cold wave activities in East Asia during El Nino (La Nina) winter. In other words, the cycle of anomalous strong winter monsoon (cold waves) and anomalous weak winter monsoon in East Asia, which has interannual time scale, is probably link up with the ENSO cycle.

III. Reduced Trade Wind over the Equatorial Western Pacific Caused by Strong Winter Monsoon in East Asia

The weakened trade wind have been regarded as an important origin of El Nino event, especially the westerly bursts over the equatorial western Pacific. In this section, the data analyses will show that the equatorial westerly bursts are closely related to the winter monsoon (activities of cold wave) in East Asia.

At first, we comparisonally analyzed the situations prior to El Nino event in 1986 and La Nina in 1988. The time-longitudinal sections of zonal wind at 850hPa averaged in 5°S-5°N latitudes are shown in Fig.2, respectively for the cases in 1986 and 1988. It is very clear that there are stronger westerlies prior to the occurrence of El Nino in 1986 (during 1985-1986 winter and 1986 spring)

over the equatorial western Pacific (110°E-160°E); but prior to the La Nina in 1988, there are obvious easterlies after January 1988. This means the positive (negative) anomalies of equatorial westerly over the equatorial western Pacific are closely related to the occurrence of El Nino (La Nina). Corresponding to the Fig.2, the time-longitudinal sections of meridional wind at 850hPa averaged in 30°N-35°N latitudes are give in Fig.3, respectively for the cases in 1986 and 1988. If there are stronger northerlies in the 110°E-135°E region, the winter monsoon should be stronger in East Asia. It is clearly shown in Fig.3 that there are stronger winter monsoon in East Asia prior to the occurrence of El Nino event in 1986, but weaker winter monsoon in East Asia prior to La Nina in 1988.

Above-mentioned results shown not only the relationship between winter monsoon in East Asia and the anomalies of the equatorial westerlies over the western Pacific but also their possible excitation effect to ENSO. The following analyses will point out the enhancements of the winter monsoon and equatorial westerlies over the western Pacific are all corresponding to the intrusions of cold wave in East Asia as shown in Fig.4. The Fig.4a and Fig.4b given the temporal variations of the surface pressure and the surface air temperature at Beijing and Jinan during December 1975 - January 1976, respectively; The obvious decrease of temperature and increase of the pressure at the same time can express an intrusion of cold wave in East Asia and marked in letter "c". The Fig.4c shows the temporal variation of meridional wind at 850hPa in (20°N,115-140°E) region and the arrows express the enhancement of the northerlies (winter monsoon). The Fig.4d shows the temporal variation of zonal wind at 850hPa in (0°,135°-160°E) region and the arrows express the westerly anomalies over the equatorial western Pacific. It is very clearly shown in Fig.4 that there are always weakness of the trade wind (westerly burst) over the equatorial western Pacific after each stronger cold wave and each enhancement of winter monsoon in East Asia.

The impact of stronger winter monsoon on the westerly anomalies over the equatorial western Pacific is also clearly shown during the TOGA-COARE observation. In December 1992 - February 1993, there are twice westerly bursts over the equatorial western Pacific area, correspondingly, two stronger cloud waves and aerotroughs intruded southwards into East Asia and stronger winter monsoon were caused. From the temporal variations of the geopotential heights at 500hPa in (30°N, 125°-135°E) and the surface pressure and temperature at Shanghai, it can be shows in Fig.5a and Fig.5b that there are stronger cold

waves in 8-12 December, 1992 and 13-18 January, 1993 in East Asia. Two westerly anomalies were both observed at Kexue 1# (4°S, 156°S) and Nauru (0.54°S, 166.92°E) in 17 December, 1992 - 7 January, 1993 and in 26 January - 16 February, 1993 (Fig.5c and Fig.5d). The westerly anomalies appear after the southward intrusions of stronger cold wave in East Asia, and the westerly anomalies at Kexue 1# are longer than at Nauru.

Therefore, the observations (including TOGA-COARE observations) all shown that stronger cold waves and winter monsoon in East Asia can reduce the trade wind and produce the westerly anomalies (bursts) over the equatorial western Pacific. It has been indicated that anomalous westerlies over the equatorial western Pacific can excite anomalous oceanic Kelvin wave, which has been regarded an important factor to cause El Nino event. In other words, the westerly anomalies over the equatorial western Pacific caused by anomalous winter monsoon in East Asia is an important factor to excite ENSO through anomalous oceanic Kelvin wave and coupling air-sea interaction.

IV. Strong Convection and Intraseasonal Oscillation over the Equatorial Western Pacific Caused by Strong Winter Monsoon in East Asia

As we know, the rainfall is mainly convectional in the tropics, the precipitation is able to represent convective activity. At first, we will be shown the anomalous precipitation (strong convection) associated the El Nino events in the equatorial western Pacific area based on the climate analyses.

The strong convection over the equatorial western Pacific and anomalous winter monsoon in East Asia prior to El Nino event are shown in Table 2. Here ΔT_s is averaged surface air temperature anomalies at Ishigakijima (24°20'N,124°10'E) and Minamidaitojima (25°50'N,131°14°E) in the wintertime, the negative anomalies represented stronger winter monsoon in East Asia; ΔR is precipitation anomalies at Truk, Caroline Islands (7°28'N,151°51'E), positive anomalies can basically represented strong convection activities over the equatorial western Pacific. It is clear that there are stronger cumulus convection and positive precipitation anomalies over the equatorial western Pacific corresponding to stronger winter monsoon in East Asia. The smaller negative anomaly of the precipitation in November 1981-April 1982 shown in Table 2 may be a result due to eastward movement of the maximum rainfall, because the OLR data show that there are very strong negative anomalies over the equatorial centre-western Pacific in November 1981-April 1982.

Table 2 The winter monsoon anomalies in East Asia and the precipitation anomalies at Truk, Caroline in the wintertime prior to the occurrence of El Nino event

	1962.11 | 1963.4	1964.11 | 1965.4	1967.11 | 1968.4	1971.11 | 1972.4	1975.11 | 1976.4	1981.11 | 1982.4	1985.11 | 1986.4
ΔT_s(°C)	-8.3	-2.7	-7.7	-1.5	-1.5	-2.2	-4.4
ΔR(mm)	209	150	544	51	223	-34	347

In order to illustrate strong convection over the equatorial western Pacific caused by strong winter monsoon in East Asia, the distributions of correlation coefficients between the TBB and the aerotrough at 500 hPa over East Asia are given in Fig.6. The temperature of black body at cloud top (TBB) received at the satellite can represent the intensity of convective activity very well, and the aerotrough activity over East Asia will directly lead to outbreak of cold wave and enhance winter monsoon in East Asia. Here, the aerotrough activity is expressed by using the averaged height at 500hPa in (30°-45°N, 125°-145°E) region. It is clearly shown in Fig.6 that there is obvious relationship between convective activity over the equatorial western Pacific and the aerotrough activity in East Asia, strong convections are associated with strong aerotrough and the strong convections over the equatorial western Pacific lag the deepening of aerotrough over East Asia for 5-10 days.

According to the theoretical analyses[5-7], stronger cumulus convection over the equatorial western Pacific should excite stronger intraseasonal oscillation through the wave-CISK mechanism. In can be also proved by using data analyses. In Fig.7, the temporal variations of 30-60 day band-pass filtered u^2 (can be regarded as kinetic energy) at 200hPa for different latitudes over the northwestern Pacific are given. Over the equatorial western Pacific, the intraseasonal oscillations are exceedingly strengthened (maximum kinetic energies) during the springs in 1982 and 1986 prior to the occurrence of corresponding El Nino events (Fig.7c). Additionally it can be found that before the tropical intraseasonal oscillations are strengthened over the equatorial western Pacific, the 30-60 day oscillations in the middle latitudes over the northwestern Pacific and East Asia have been strengthened in advance (Fig.7a-b). This shows not only shown possible exciting effect of stronger tropical intraseasonal oscillation (especially over the equatorial western Pacific) to the occurrence of El Nino event, but also the influence of the winter monsoon in East Asia on the enhancement of intraseasonal oscillation over the equatorial western Pacific.

V. Anomalous Intraseasonal Oscillation Exciting ENSO Mode

The exciting effect of stronger intraseasonal oscillation in the tropics to the El Nino event, which can be regarded as a very low-frequency oscillation or a quasi-stationary system in the tropical atmosphere because its mean period is about 3-4 years, can be also shown by using analyzing kinetic energy transfer of tropical atmospheric systems. The temporal variations of kinetic energies at 200hPa for intraseasonal (30-60 day) oscillation and quasi-stationary system (period>90 day) in the tropical atmosphere are given in Fig.8 and Fig.9, corresponding to the occurrences of the 1982-1983 El Nino and the 1986-1987 El Nino respectively. It is very clear that the kinetic energies of 30-60 day oscillation in the tropical atmosphere decrease abruptly associated with the occurrence of El Nino events (June-July, 1982 and 1986); but the kinetic energies for the quasi-stationary system (including the ENSO cycle) increase abruptly in the same time. The disappearance and increase of kinetic energies mean a transfer of kinetic energy from 30-60 day low-frequency oscillation to quasi-stationary system, so that the El Nino event can be induced through the sea-air interaction.

How anomalous intraseasonal oscillation can excite El Nino event? Based on a simple dynamical analysis, we investigated a possible mechanism. A tropical air-sea coupled model can be written as follows from Gill's atmospheric model (1980)[8] and Philander's oceanic model (1984)[9]:

$$D\frac{\partial U}{\partial x} = -\eta(h - \kappa h^3) - F \tag{1}$$

$$\frac{\partial u}{\partial t} + u\frac{\partial u}{\partial x} + g\frac{\partial h}{\partial x} = \gamma U \tag{2}$$

$$\frac{\partial h}{\partial t} + u\frac{\partial h}{\partial x} + (d+h)\frac{\partial u}{\partial x} = 0 \tag{3}$$

where U is zonal wind, D is atmospheric equivalent depth; u is zonal current in the ocean, d is equivalent depth of oceanic mixed layer and h is deviation from d; $\eta(h - \kappa h^3)$ is parameterized heat flux from the ocean to atmosphere, γU is the wind stress of the atmosphere to the ocean, F is an atmospheric forcing.

Selecting time scale $T=L/c_0$, where L is basin width of the ocean, c_0 is the Kelvin wave speed in the ocean, the nondimensional coupled equations can be written:

$$\frac{\partial U}{\partial x} + \eta_1 h = \eta_1 \kappa h^3 - \eta_2 F \tag{4}$$

$$\frac{\partial u}{\partial t} - \gamma_1 U + u\frac{\partial u}{\partial x} + \frac{\partial h}{\partial x} = 0 \tag{5}$$

$$\frac{\partial h}{\partial t}+\frac{\partial u}{\partial x}+\frac{\partial}{\partial x}(uh)=0 \tag{6}$$

where $\eta_c=\eta+\frac{c_0^2}{c_a^2}$, $\gamma_c=\gamma T$, $\eta_2=T/D$, c_a is gravity wave speed in the atmosphere.

Solving the coupled equations (4)-(6), the air-sea coupled mode can be obtained for different cases:

If there is no forcing (F=0), the air-sea interaction system is a self-organised system, the coupled modes are periodical oscillations depending on the coupling intensity. Some evolutions of the amplitude of coupled mode with different coupling intensity are shown in Fig.10. It is shown that the period is longer when the coupling interaction is stronger, but an oscillation with mean time-scale like ENSO (about 4 years) can be excited in the air-sea coupled system and means the air-sea interaction is an important base to produce ENSO. As we know, an obvious feature of ENSO represented by SSTA in the equatorial centre-eastern Pacific is its nonperiodicty with different evolution pattern. Therefore, the air-sea coupled oscillation is not the ENSO yet.

If there is a forcing, such as an biennial atmospheric forcing, the coupled modes with different period and different pattern will be excited in the air-sea interaction system, as shown in Fig.11. This means the atmospheric forcing can excite a coupled modes, remarkable which like ENSO cycle, in the air-sea interaction system. In other words, interannual variation of tropical intraseasonal oscillation caused by anomalous winter monsoon, as an atmospheric forcing on the air-sea interaction system, is favourable to excite coupled modes like ENSO cycle.

Above-mentioned discussions have obviously shown that stronger winter monsoon in East Asia in the wintertime can exceedingly enhance the cumulus convection and intraseasonal oscillation over the equatorial western Pacific, and then it can play an important role in the occurrence of El Nino event.

VI. The Winter Monsoon in East Asia in El Nino/La Nina Year

It has been indicated in our previous studies that the winter monsoon in East Asia is usually weaker in El Nino year[10]. And the reasons to cause weaker East Asian winter monsoon in El Nino year are also investigated, i.e., the stronger positive anomalies of SST in the equatorial eastern Pacific can enhance the westerlies in middle latitudes and negative SSTA in the equatorial

western Pacific can lead to the polar front to north side in East Asia, so that the southward intrusion of cold waves in East Asia is unfavourable in El Nino year[11].

Here, we only give some simple discussions to prove previous conclusion. Table 3 shows the monthly mean surface air temperature anomalies (°C) in El Nino winter (Nov.-Feb.) averaged at Shenyang, Beijing, Qingdao, Wuhan Shanghai, Fuzhou and Guangzhou for 21 El Nino events from 1900-1992. It is clear that there are higher temperature in eastern China in most of El Nino winters (~75%). In other words, El Nino event could reduce the winter monsoon in East Asia. In order to compare with above results, the cases in relation to La Nina are also analyzed. It is shown that the cold waves (winter monsoon) in East Asia are stronger in La Nina winter.

Table 3 Monthly mean anomalies of the surface air temperature (°C) in eastern China in El Nino winter (Nov.-Feb.)

Time	1911-1912	1913-1914	1918-1919	1923-1924	1925-1926	1930-1931	1935-1936
	0.5	0.6	-0.05	0.6	0.8	-0.05	-1.2
Time	1940-1941	1944-1945	1948-1949	1951-1952	1953-1954	1957-1958	1963-1964
	1.0	/	1.0	0.8	0.9	0.3	-0.3
Time	1965-1966	1968-1969	1971-1972	1976-1977	1982-1983	1986-1987	1991-1992
	0.8	-0.05	0.8	-1.6	0.8	0.9	1.0

In Fig.12, the time-longitudinal distributions of meridional wind anomaly in (20°-30°N) latitudes at 850hPa during Oct. 1982 - Jun. 1983, Oct. 1986 - Jun. 1987 and Oct. 1988 - Jun. 1989 are shown. It is clear that there are southerly (positive) anomalies in (110°-160°E) region, which represent weak winter monsoon, during El Nino winter; and there is northerly (negative) anomalies in (110°-160°E) region, which represents strong winter monsoon, during La Nina winter.

Temporal variation of monthly surface air temperature anomalies averaged at Qingdao, Zhenzhou, Hefei, Shanghai, Wenzhou, Fuzhou, Ganzhou and Guangzhou during 1951-1984 is given in Fig.13. It is also obvious that the temperature in eastern China are all higher in El Nino winter except in 1976-1977 winter and means there are weaker winter monsoon during El Nino winter. We can also find there are lower temperature (stronger winter monsoon) in East Asia prior to the occurrence of El Nino events. In other words, corresponding to El Nino event, the surface air temperature in East Asian usually shows a great

change from stronger negative anomalies in last winter to stronger positive anomalies in El Nino winter; the winter monsoon in East Asia also shows a great change from stronger to weaker.

VII. Influences of El Nino on Intraseasonal Oscillation in the Tropical Atmosphere

In the above two sections, the exciting effect of the winter monsoon to the El Nino event, through reducing trade wind and enhancing cumulus convection and intraseasonal oscillation over the equatorial western Pacific, is obviously shown. Some influences of El Nino on intraseasonal oscillation in the tropical atmosphere will be discussed in this section.

In Fig.14, the temporal variation of 30-60 day band-pass filtered u^2 at 200hPa over the equatorial centre-eastern Pacific is shown and it is clear that the u^2, which can be regarded as kinetic energy of intraseasonal oscillation, are weaker during El Nino. This situation is still found over the equatorial centre-western Pacific region or in the cases and at 500hPa and 850hPa levels. Therefore, it can be concluded that the El Nino has a reducing effect on the intensity of intraseasonal oscillation in the tropical atmosphere.

The outgoing longwave radiation (OLR) is an efficient physical quantity used to investigate the activity of intraseasonal oscillation in the tropical atmosphere. The temporal variation of 30-60 day band-pass filtered OLR over the equatorial western Pacific is shown in Fig.15, the weaker amplitudes are clearly declared during September 1982 - March 1984, especially in the period from September 1982 to August 1983. As we know, a stronger El Nino event occurred in 1982-1983, therefore, the analyses in OLR data also shown that the El Nino has a reducing effect to the intensity of intraseasonal oscillation in the tropical atmosphere.

In order to investigate further the influence of El Nino on intraseasonal oscillation in the tropics, numerical experiments are completed by using a CSIRO-GCM4, which is a 4-level GCM with a rhomboidal wavenumber 21 spectral representation[12]. One experiment is control run (CE) in which the SST was climatological data with temporal variation; another is anomalous experiment (AE) in which the SST was observational data in 1983. The Fig.16 shown the longitudinal distributions of kinetic energy of tropical intraseasonal oscillation in the upper troposphere obtained in CSIRO-GCM4 for the CE and AE, respectively. It is very clear that the kinetic energy of tropical intraseasonal

oscillation obtained in AE is smaller than that in CE for either the zonal mean or the maximum. The numerical simulations in GCM also shown that intraseasonal oscillation in the tropical atmosphere will be reduced in the El Nino condition.

As we know, the vertical structure of intraseasonal oscillation in the tropical atmosphere shows a baroclinic feature and its wind field/pressure field change the sign from the lower to the upper troposphere. The Fig.17a is an example which shows longitudinal distribution of geopotential heights of intraseasonal oscillation along 10°S-10°N latitudes in 1981 summer. It is clear that the major trough (ridge) at 850hPa is corresponding to the major ridge (trough) at 200hPa, the baroclinic structure feature is shown. On the contrary in 1982 summer, either geopotential height or zonal wind (Fig.17b) shows that the vertical structure of intraseasonal oscillation is inclined to be barotropic, though the El Nino event just began in 1982 summer.

The numerical experiments in GCM above-mentioned also clearly shown the influence of El Nino on the structure of intraseasonal oscillation in the tropical atmosphere. The Fig.18a shows longitudinal distributions of the simulated surface pressure and temperature (geopotential height is similar) at the upper troposphere of intraseasonal oscillation in the tropical atmosphere for the CE case, and it clearly reflected general baroclinic feature. But for the AE case (Fig.18b), the simulated intraseasonal oscillation tends to barotropic feature. In other words, the El Nino condition in GCM also lead the tropical intraseasonal oscillation to incline to barotropic structure.

VIII. Conclusions

In this paper, the interactions between anomalous winter monsoon in East Asia and ENSO are further studied systematically. The strong (weak) anomaly of winter monsoon in East Asia can play an important role in excitation of El Nino (La Nina) through reducing (enhancing) trade wind and enhancing (weakening) cumulus convection (intraseasonal oscillation) over the equatorial western Pacific. After the occurrence of El Nino (La Nina), intraseasonal oscillation in the tropical atmosphere and winter monsoon in East Asia will all be reduced (enhanced). In other words, there are two cycles, i.e. ENSO cycle; anomalous strong and weak winter monsoon cycle in East Asia, which has interannual time scale. And these two cycles are closely linked up each other.

Based on the analyses in this paper, we can suggest a schematic diagram of the interactions between ENSO cycle and anomalies of winter monsoon in

East Asia as showing in Fig.19.

It should be indicated that the monsoon (especially winter monsoon) in East Asia, Intraseasonal oscillation in the tropical atmosphere and ENSO are closely related and interactive each other; we can caricature them as showing in Fig.20. Their relationship is very important to the climate variation and need to be studied systematically. At least it includes the air-sea interaction, the middle-low latitude atmospheric interaction and the interaction between the different time-scale climate variations.

We would like to say that the anomaly of cold wave activity in the southern Pacific, such as the anomaly of winter monsoon in Australia, can also probably pay a certain role in the occurrence of ENSO. But according to our preliminary analyses, the anomalies of winter monsoon in East Asia are more important to ENSO cycle.

References

[1] Li Chongyin, 1988: Frequent activities of stronger aerotroughs in East Asia in wintertime and the occurrence of the El Nino event. *Science in China* (Series B), 31, 976-985.

[2] Li Chongyin, 1990: Interaction between anomalous winter monsoon in East Asia and El Nino events, *Adv. Atmos. Sci.*, 7, 36-46.

[3] Webster, P.J., and S. Yang, 1992: Monsoon and ENSO: Selectively interactive systems, *Quart. J.R. Meteoro. Soc.*, 118, 877-926.

[4] Yasunari, T., and Y. Seki, 1992: Role of the Asian Monsoon on the interannual variability of the global climate system. *J. Meteor. Soc. Japan*, 70, 177-189.

[5] Li Chongyin, 1985: Action of summer monsoon troughs (ridges) and tropical cyclones over South Asia and the moving CISK mode, *Scientia Sinica (B)*, 28, 1197-1207.

[6] Lau, K.M., and L. Peng, 1987: Origin of low-frequency (intraseasonal) oscillation in the tropical atmosphere, Part I: The basic theory, *J. Atmos. Sci.*, 44, 950-972.

[7] Li Chongyin, 1990: Dynamical study on 30-60 day oscillation in the tropical atmosphere outside equator, *Chinese J. Atmos. Sci.*, 14, 101-112.

[8] Gill, A.E., 1980: Some simple solutions of heat induced tropical circulation, Q.J.R. Meteor. Soc., 106, 447-462.

[9] Philander, S.G.H., T. Yamagaata and R.C. Pacanowski, 1984: Unstable air-sea interactions in the tropics, J. Atmos. Sci., 41, 604-613.

[10] Li Chongyin, 1989: Warmer winter in eastern China and El Nino, *Chinese Science Bulletin*, 34, 1801-1805.

[11] Wu Zhengxian, Li Chongyin, Chen Biao, Wu Guoxiong, 1990: A diagnostic analysis of general circulation anomaly during the El Nino process for the winter 1982/83, *Journal of Tropical Meteorology*, 6, 253-264.

[12] Hunt, B.G., and H.B. Gordon, 1989: Diurnally varying regional climatic simulations, *Inter. Journal of Climatology*, 9, 331-356.

Figure Captions

Fig.1 Time-longitudinal sections of the height anomalies at 500hPa over (20°-45°N) latitudes for warm (El Nino) case (a) and cold (La Nina) case (b) in 1980's, respectively. The intervals are ±10m, thick solid line is zero, dashed lines represent negative anomalies.

Fig.2 Time-longitudinal sections of zonal wind at 850hPa averaged in (5°S-5°N latitudes) for November 1985 - October 1986 and November 1987 - December 1988, respectively. The intervals ±3m/s, shaded area represents the westerly is greater than 6m/s.

Fig.3 Time-longitudinal sections of meridional wind at 850hPa averaged in (30°-35°N latitudes) for November 1985 - October 1986 and November 1987 - October 1988 respectively. The intervals ±2m/s, shaded area represents the northerly is greater than 6m/s.

Fig.4 Temporal variations of the surface pressure (solid line) and surface air temperature (dashed line) at Beijing (a) and Jinan (b); and the meridional wind at 850hPa averaged in (20°N,115°-140°E) region (c); and the zonal wind at 850hPa in (0°,135°-160°E) region (d) during December 1975 - January 1976.

Fig.5 Temporal variations of: (a) geopotential height at 500hPa in (30°N, 125°-135°E); (b) the surface pressure (p_s) and temperature (T_s) at Shanghai; (c) the surface wind vectors at Kexue 1# (some are partly replenished with the assimilation data at 1000hPa); (d) the surface wind vectors at Nauru.

Fig.6 The distributions of correlation coefficient between the aerotrough activities at 500hpa and TBB. a) TBB lead aerotroughs for 5 days, b) contemporary correlation, c) TBB lag aerotroughs for 5 days, d) TBB lag aerotroughs for 10 days.

Fig.7 Temporal variations of 30-60 day band-pass filtered u^2 at 200hPa in the northwestern Pacific region. a) (30°-50°N,80°-160°E) region, b) (10°-25°N,110°-180°E) region, c) (10°S-10°N,110°-180°E) region.

Fig.8 Temporal variations of zonal mean kinetic energy at 200hPa for intraseasonal oscillation (a) and the quasi-stationary system (b) in the tropical atmosphere (10°S-10°N) associated with the occurrence of El Nino in 1982.

Fig.9 Same as in Fig.3, but associated with the occurrence of El Nino in 1986.

Fig.10 The self-excited oscillations of air-sea coupled system without atmospheric external forcing. A, b and c represents coupling intensity in $1\times10^{-11}s^{-1}$, $5\times10^{-11}s^{-1}$and $1\times10^{-11}s^{-1}$, respectively.

Fig.11 The coupled modes in the air-sea interaction system with atmospheric external forcing for same coupling intensity but different forcing intensities:

Fig.12 The time-longitudinal distributions of meridional wind anomaly in (20°-30°N) latitudes at 850hPa during Oct. 1982 - June. 1893 (a), Oct. 1986 - Jun. 1987 9b) and Oct. 1988 - Jun. 1989 (c).

Fig.13 Temporal variation of monthly surface air temperature anomalies in eastern China (the data is averaged for 3 months).

Fig.14 Temporal variations of 30-60 day band-pass filtered u^2 at 200hPa in 10°S-10°N latitudes.a) 160°E-160°W region; b)130°W-11°W region.

Fig.15 Temporal variations of 30-60 day band-pass filtered OLR (w/m^2) over the equatorial western Pacific in 1982-1984.

Fig.16 Longitudinal distribution of kinetic energy (K) of the simulated intraseasonal oscillation at 350hPa in 11.1°S-11.1°N latitudes. Solid and dashed line represents the result in the CE and AE, respectively.

Fig.17 Longitudinal distributions of geopotential height in 1981 summer (a) and zonal wind in 1982 summer (b) for intraseasonal oscillation in the tropics (10°S-10°N). Solid and dashed line respectively represents 200hPa and 850hPa.

Fig.18 Longitudinal distribution of the surface pressure (solid line) and temperature at 350hPa (dashed line) of the simulated intraseasonal oscillation in the tropics (11.1°S-11.1°N) by using GCM. a) for CE results, b) for AE results.

Fig.19 Schematic diagran of the interactions between ENSO cycle and anomalies of winter monsoon in East Asia.

Fig.20 A caricature of the relationship between the monsoon in East Asia, tropical intraseasonal oscillation and El Nino.

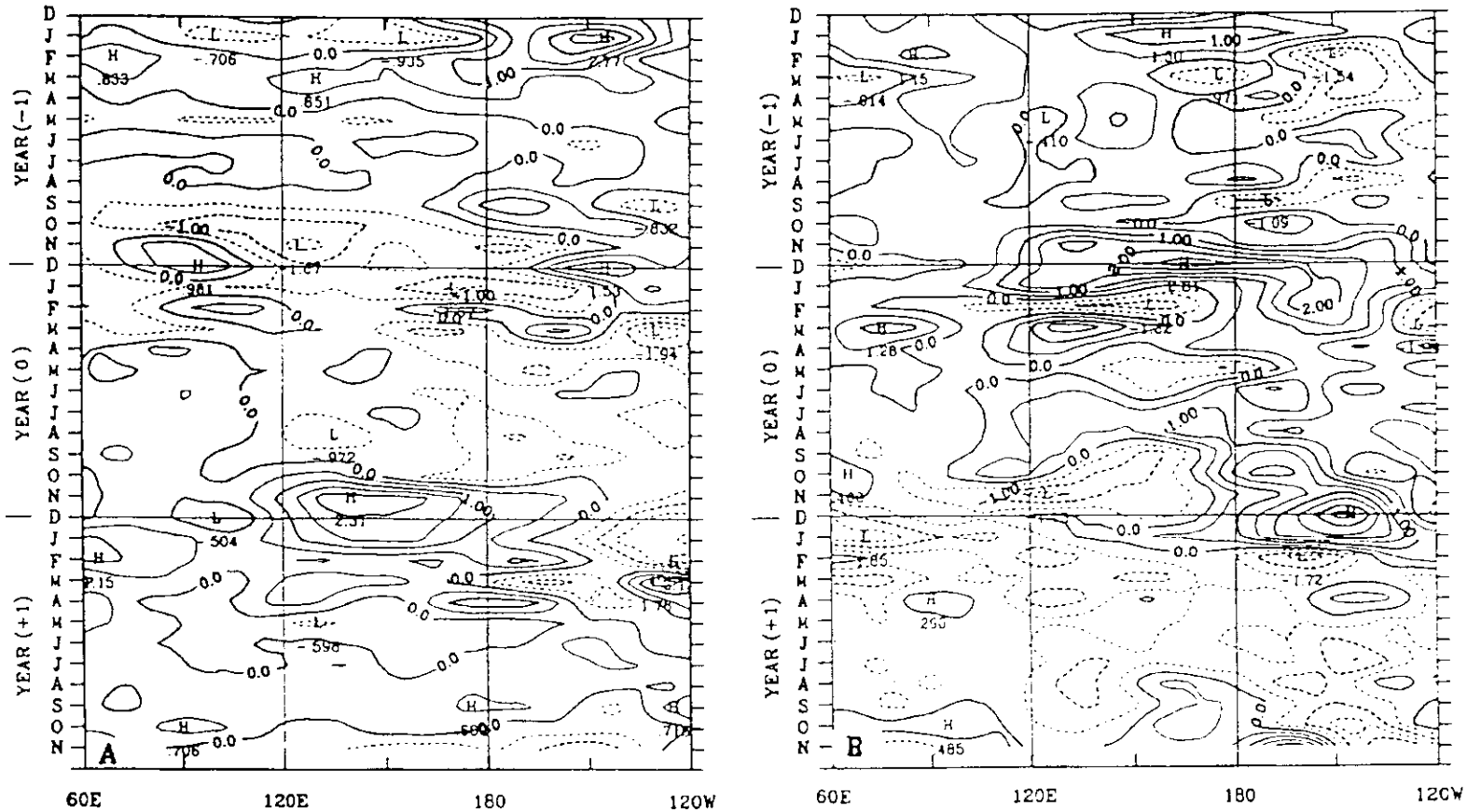

Fig.1 Time-longitudinal sections of the height anomalies at 500hPa over (20°-45°N) latitudes for warm (El Nino) case (a) and cold (La Nina) case (b) in 1980's, respectively. The intervals are ±10m, thick solid line is zero, dashed lines represent negative anomalies.

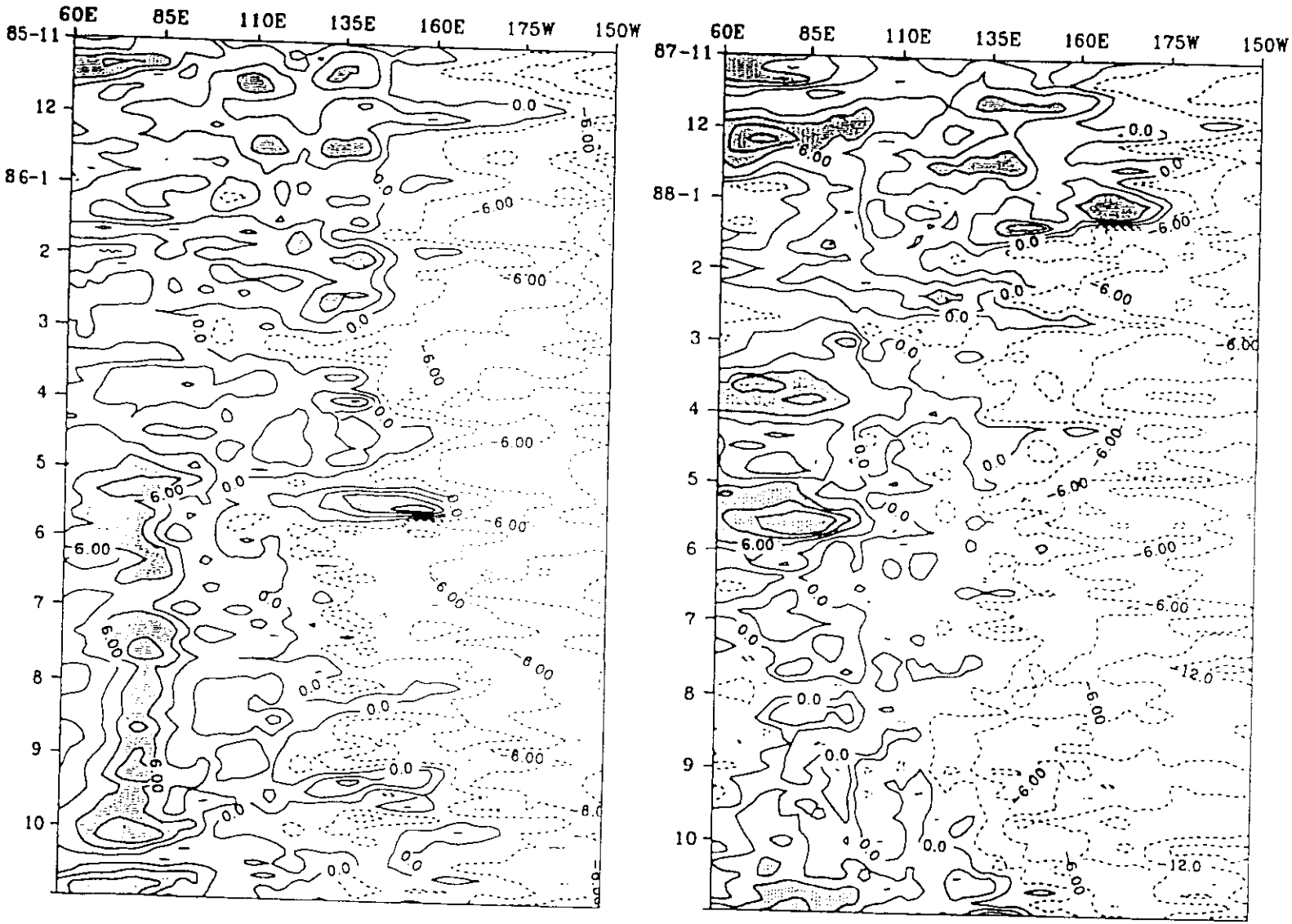

Fig.2 Time-longitudinal sections of zonal wind at 850hPa averaged in (5°S-5°N latitudes) for November 1985 - October 1986 and November 1987 - December 1988, respectively. The intervals ±3m/s, shaded area represents the westerly is greater than 6m/s.

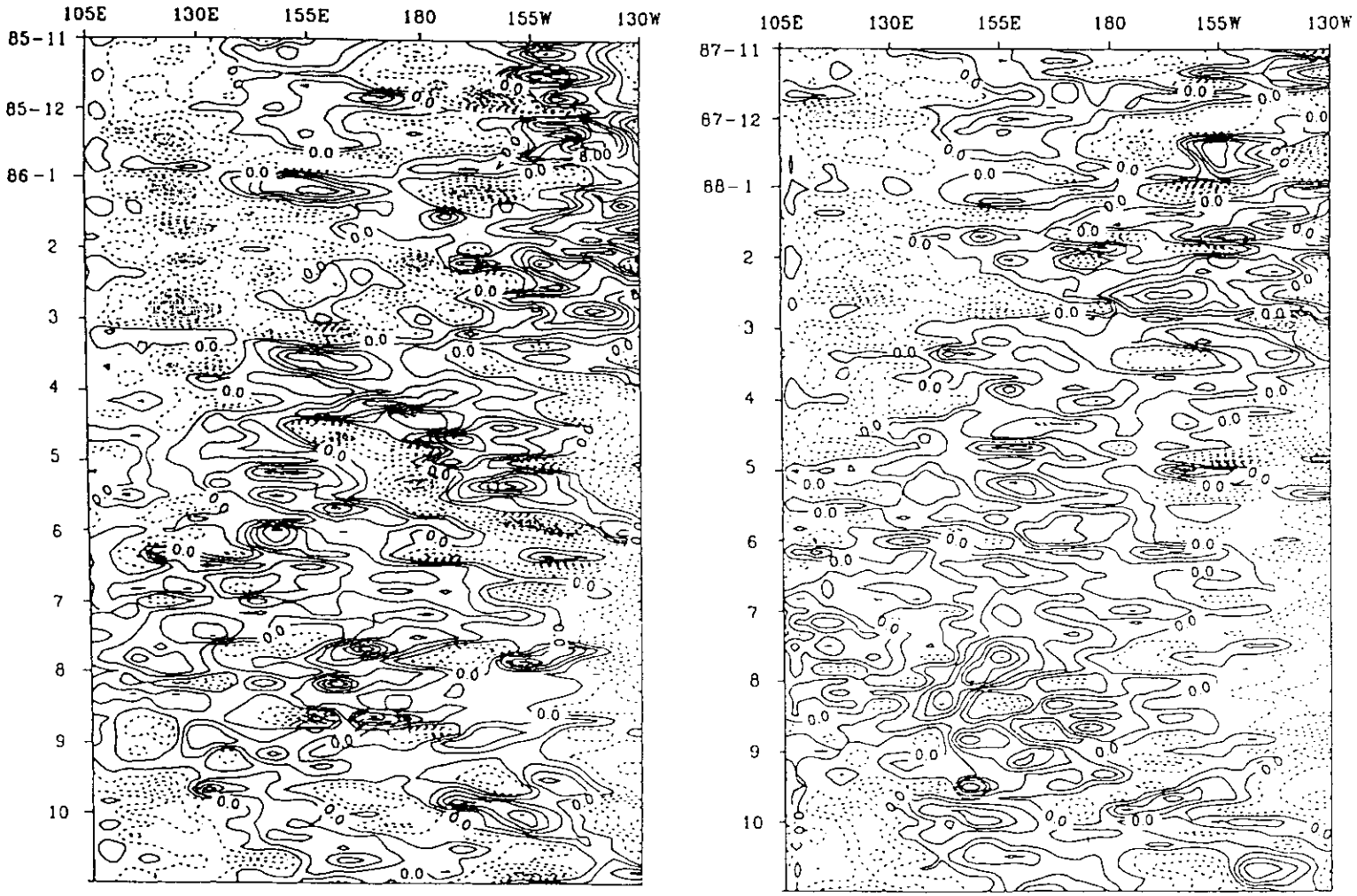

Fig.3 Time-longitudinal sections of meridional wind at 850hPa averaged in (30°-35°N latitudes) for November 1985 - October 1986 and November 1987 - October 1988 respectively. The intervals ±2m/s, shaded area represents the northerly is greater than 6m/s.

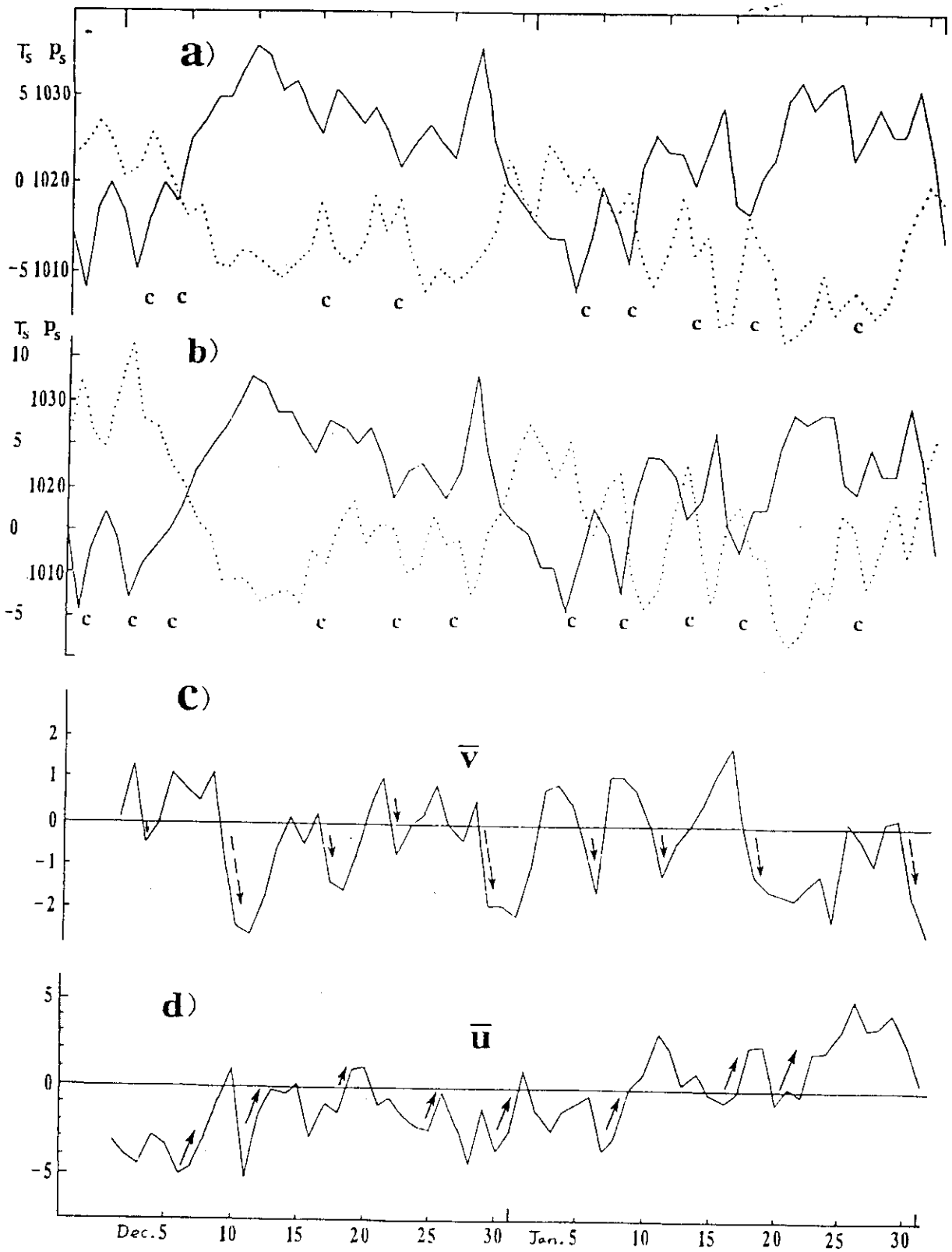

Temporal variations of the surface pressure (solid line) and surface air temperature (dashed line) at Beijing (a) and Jinan (b); and the meridional wind at 850hPa averaged in (20°N,115°-140°E) region (c); and the zonal wind at 850hPa in (0°,135°-160°E) region (d) during December 1975 - January 1976.

Fig. 11

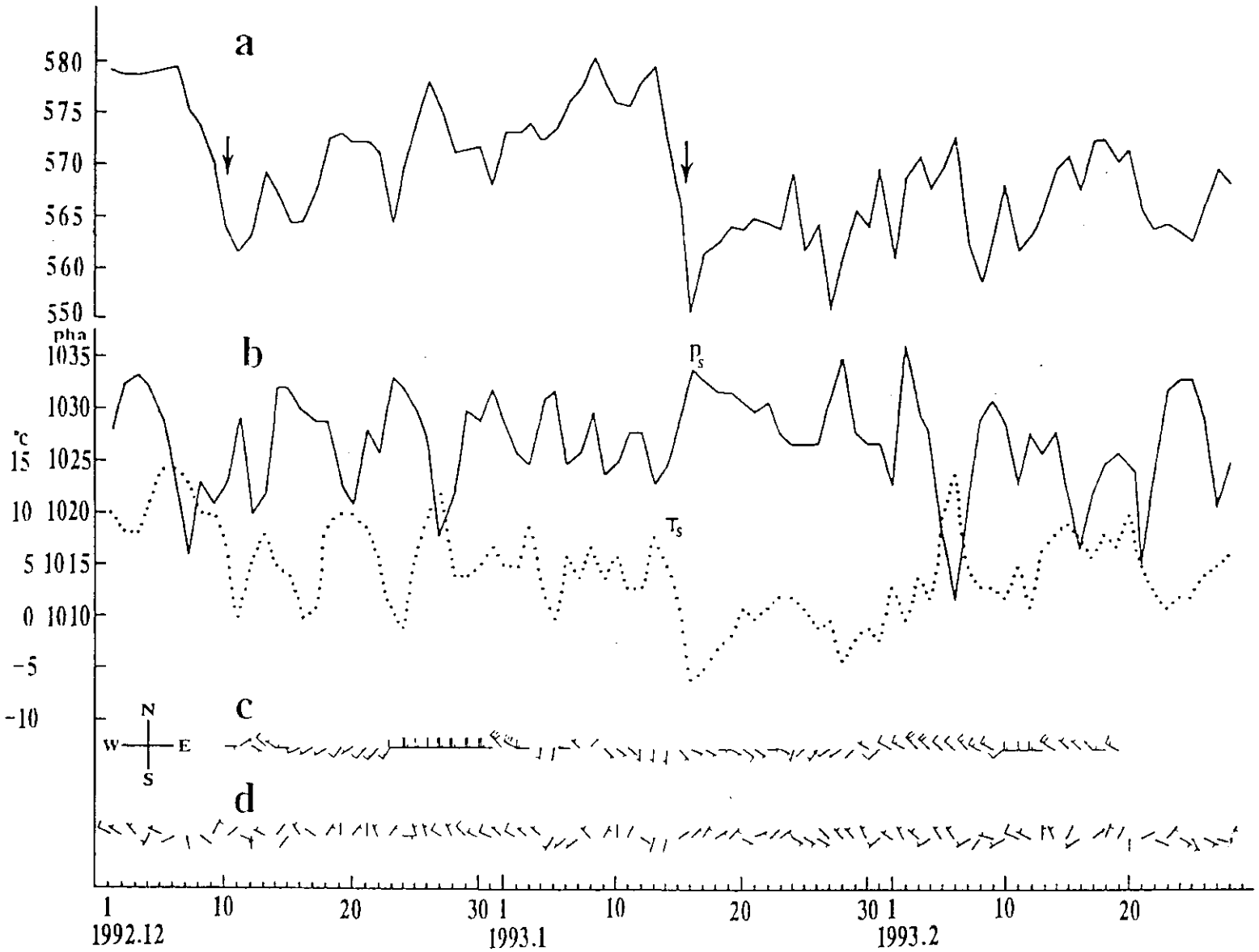

Fig.5 Temporal variations of: (a) geopotential height at 500hPa in (30°N, 125°-135°E); (b) the surface pressure (p_s) and temperature (T_s) at Shanghai; (c) the surface wind vectors at Kexue 1# (some are partly replenished with the assimilation data at 1000hPa); (d) the surface wind vectors at Nauru.

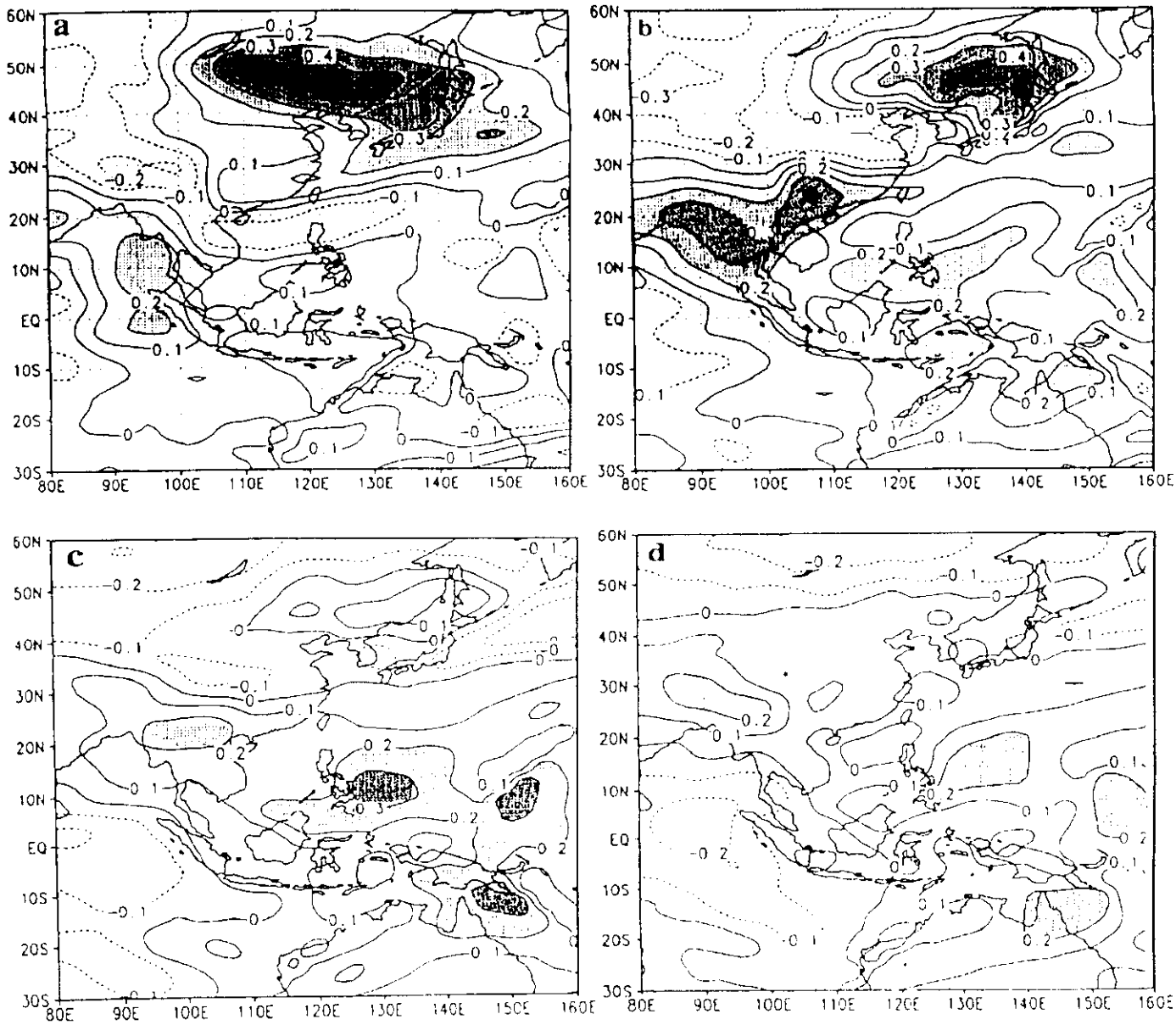

Fig.6 The distributions of correlation coefficient between the aerotrough activities at 500hpa and TBB. a) TBB lead aerotroughs for 5 days, b) contemporary correlation, c) TBB lag aerotroughs for 5 days, d) TBB lag aerotroughs for 10 days.

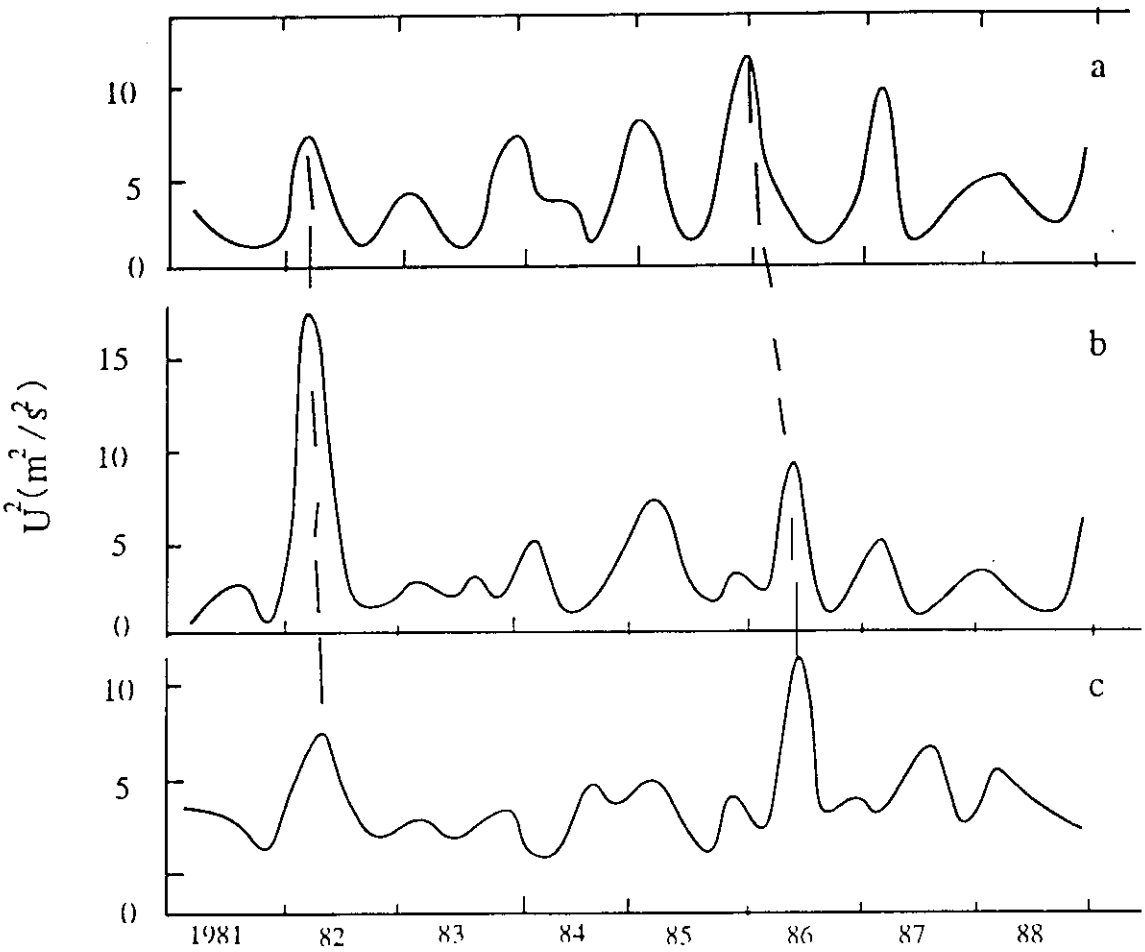

Temporal variations of 30-60 day band-pass filtered u^2 at 200hPa in the northwestern Pacific region. a) (30°-50°N,80°-160°E) region, b) (10°-25°N,110°-180°E) region, c) (10°S-10°N,110°-180°E) region.

Fig.7

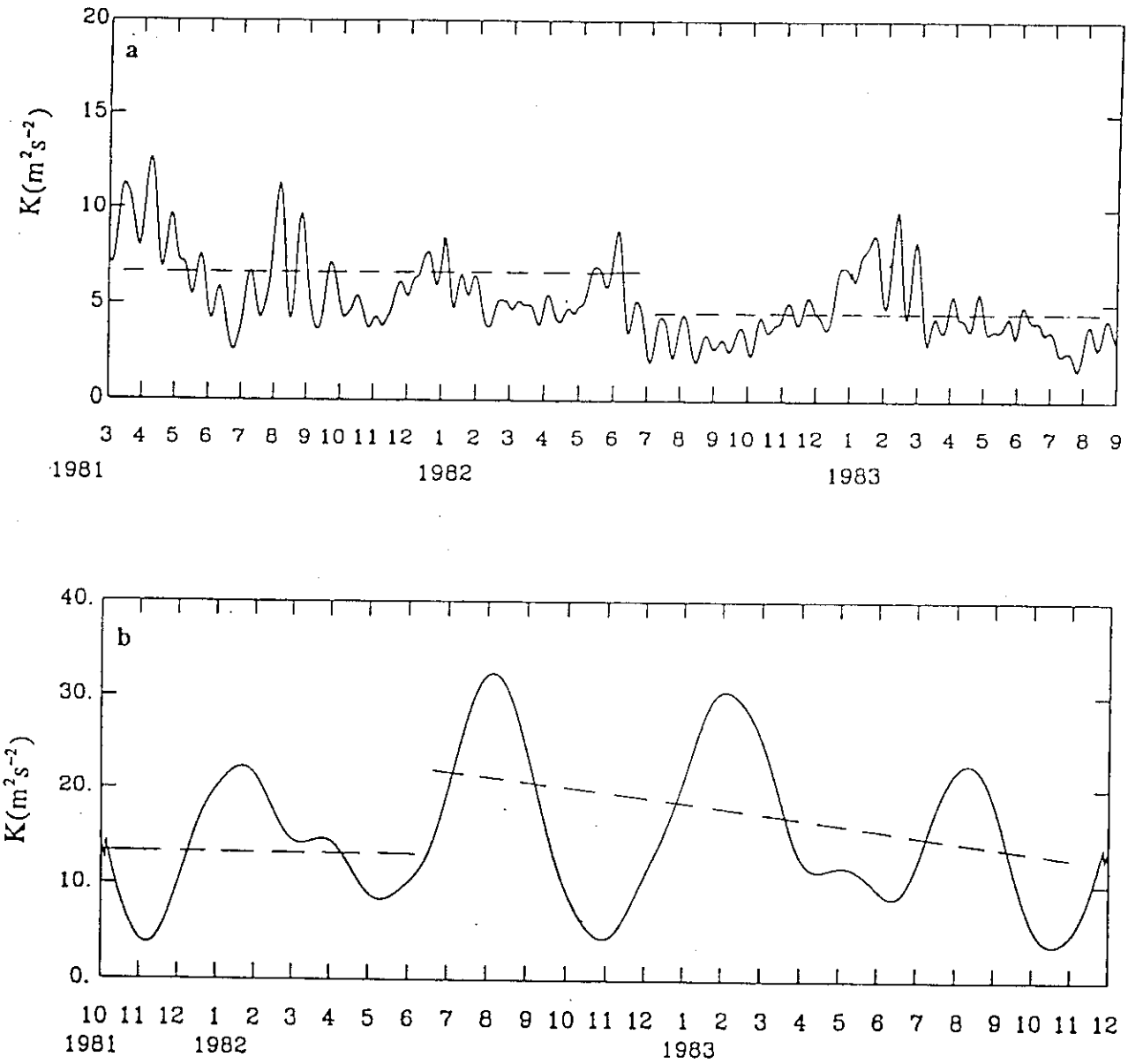

Temporal variations of zonal mean kinetic energy at 200hPa for intraseasonal oscillation (a) and the quasi-stationary system (b) in the tropical atmosphere (10°S-10°N) associated with the occurrence of El Nino in 1982.

Fig.8

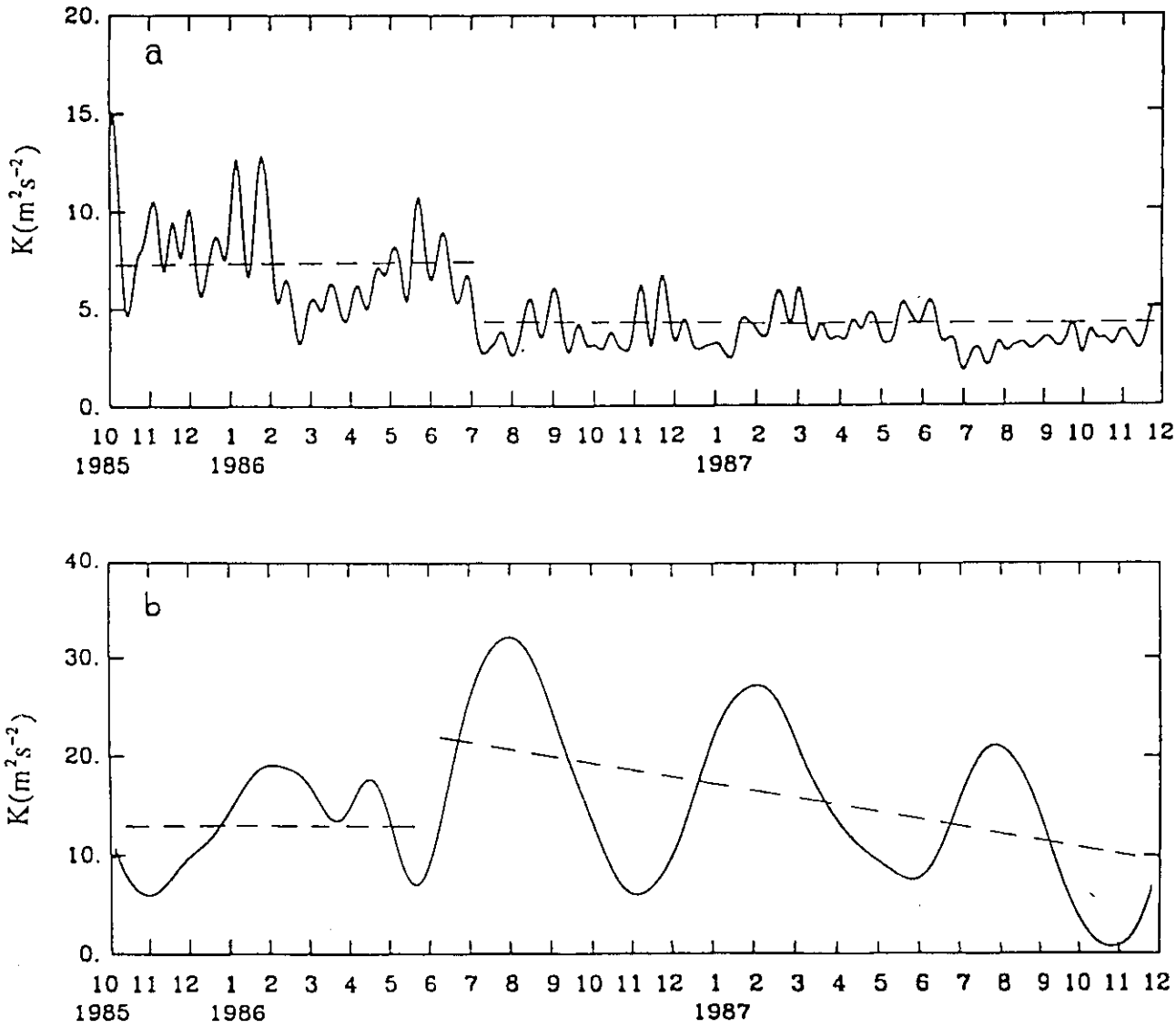

Temporal variations of zonal mean kinetic energy at 200hPa for intraseasonal oscillation (a) and the quasi-stationary system (b) in the tropical atmosphere (10°S-10°N) associated with the occurrence of El Nino in 1986.

Fig.9

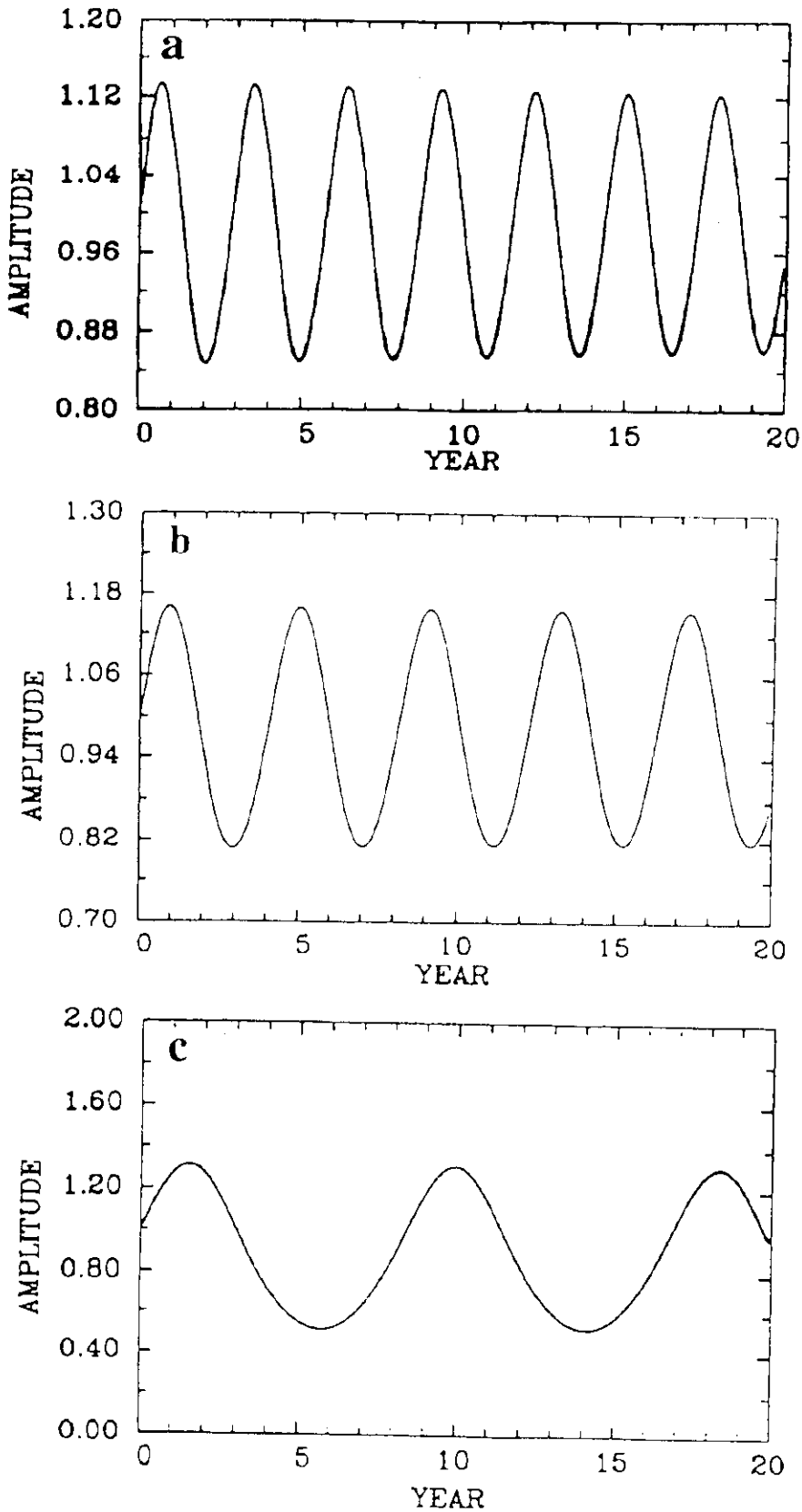

Fig.10 The self-excited oscillations of air-sea coupled system without atmospheric external forcing. A, b and c represents coupling intensity in $1\times10^{-11}s^{-1}$, $5\times 10^{-11}s^{-1}$and $1\times10^{-11}s^{-1}$, respectively.

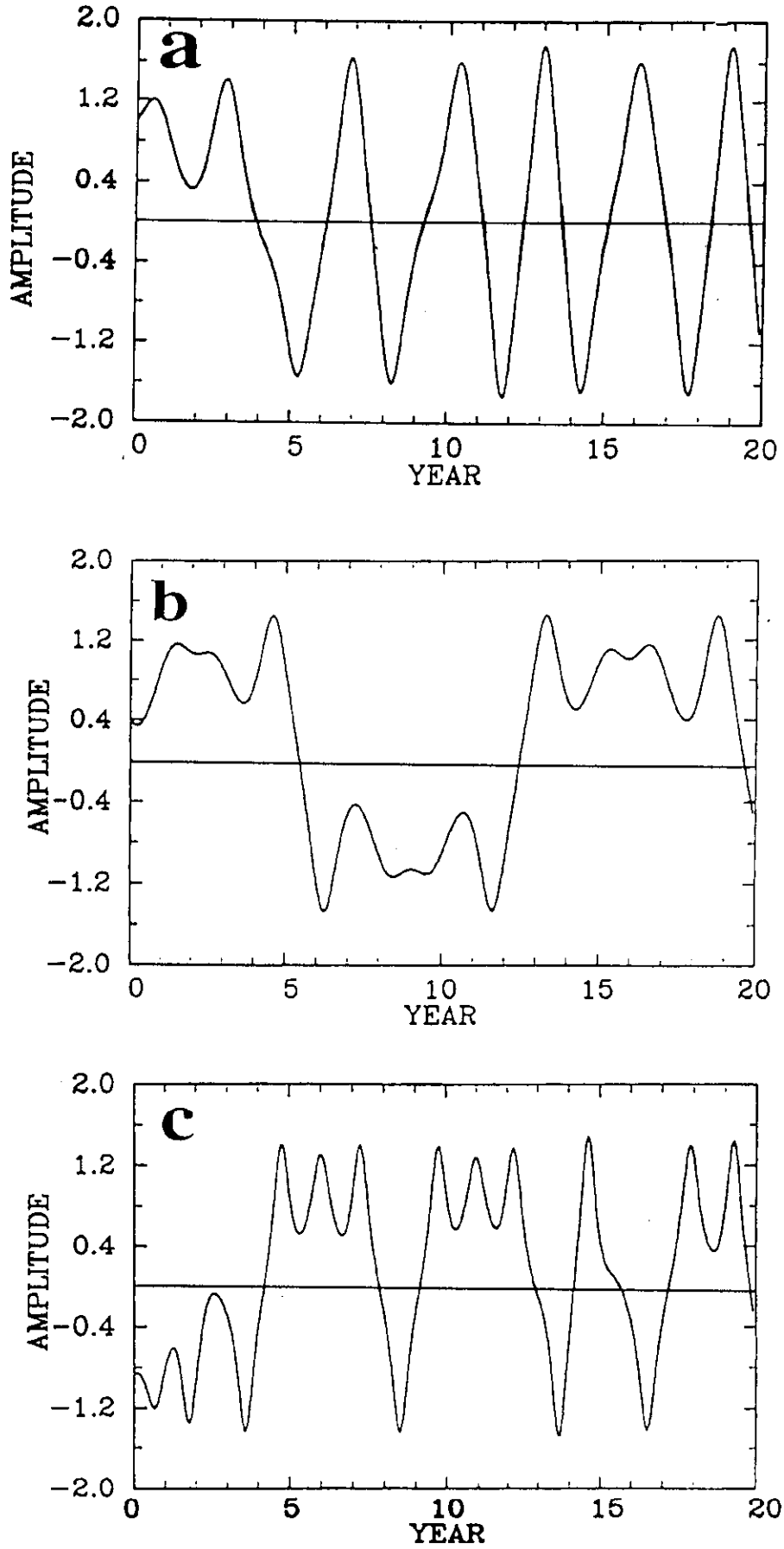

Fig.11 The coupled modes int he air-sea interaction system with atmospheric external forcing for same coupling intensity but different forcing intensities:

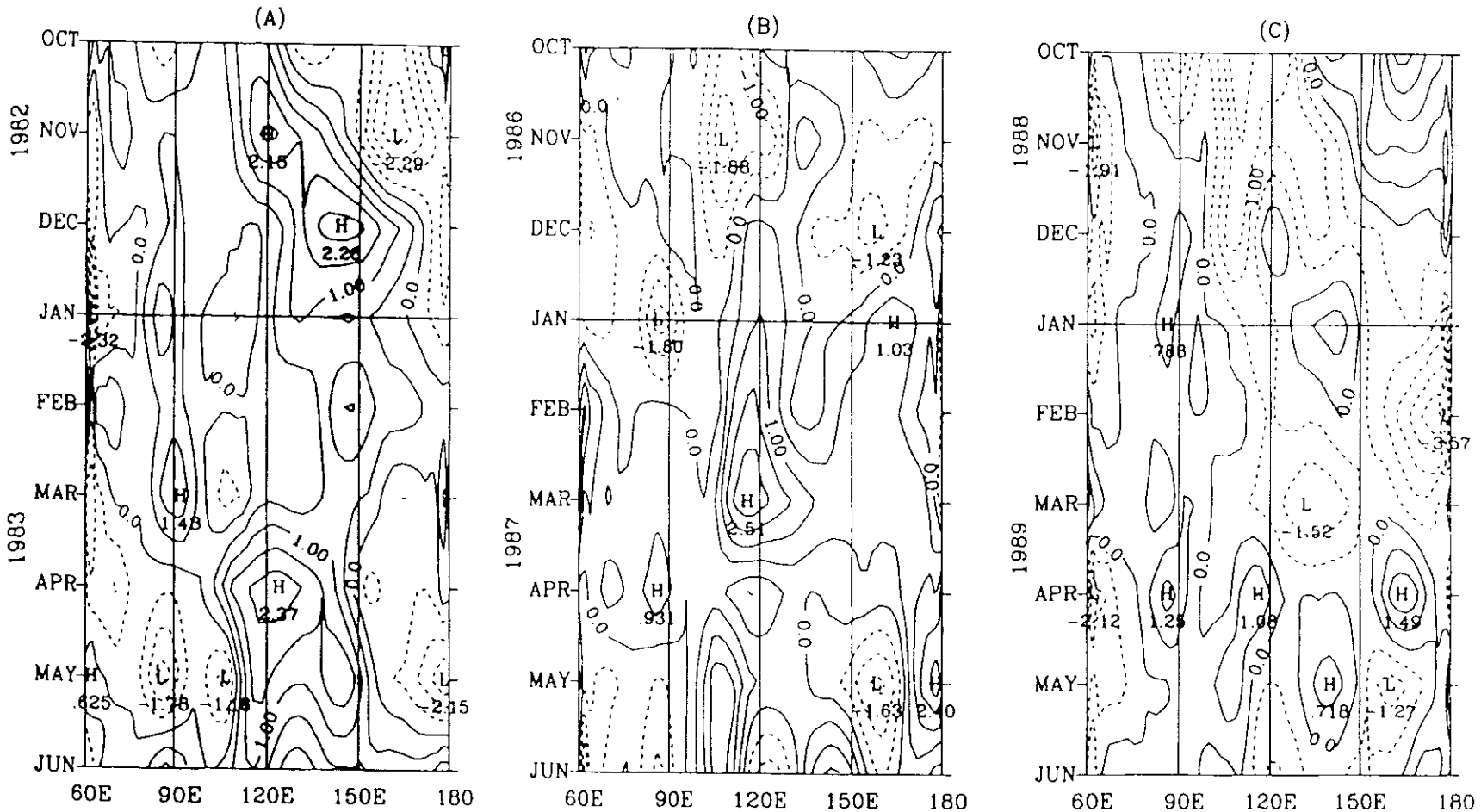

Fig.12 The time-longitudinal distributions of meridional wind anomaly in (20°-30°N) latitudes at 850hPa during Oct. 1982 - June. 1893 (a), Oct. 1986 - Jun. 1987 9b) and Oct. 1988 - Jun. 1989 (c).

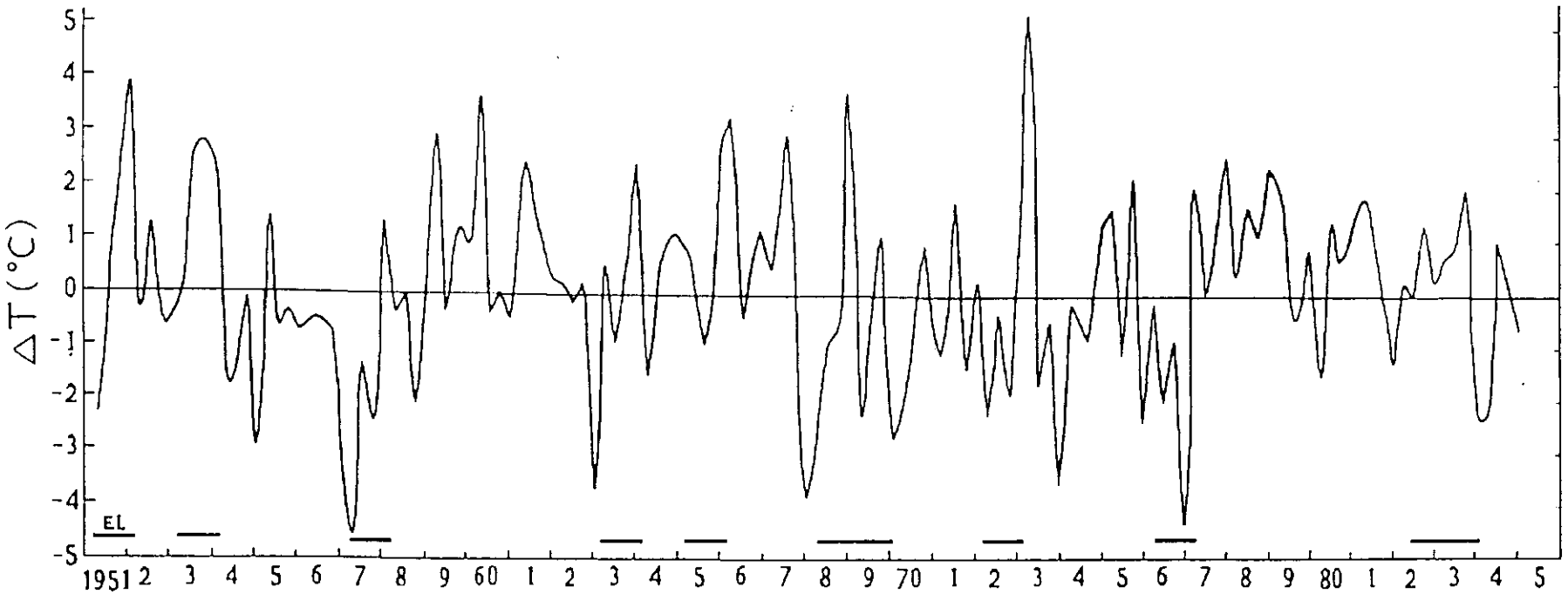

Temporal variation of monthly surface air temperature anomalies in eastern China (the data is averaged for 3 months).

Fig.13

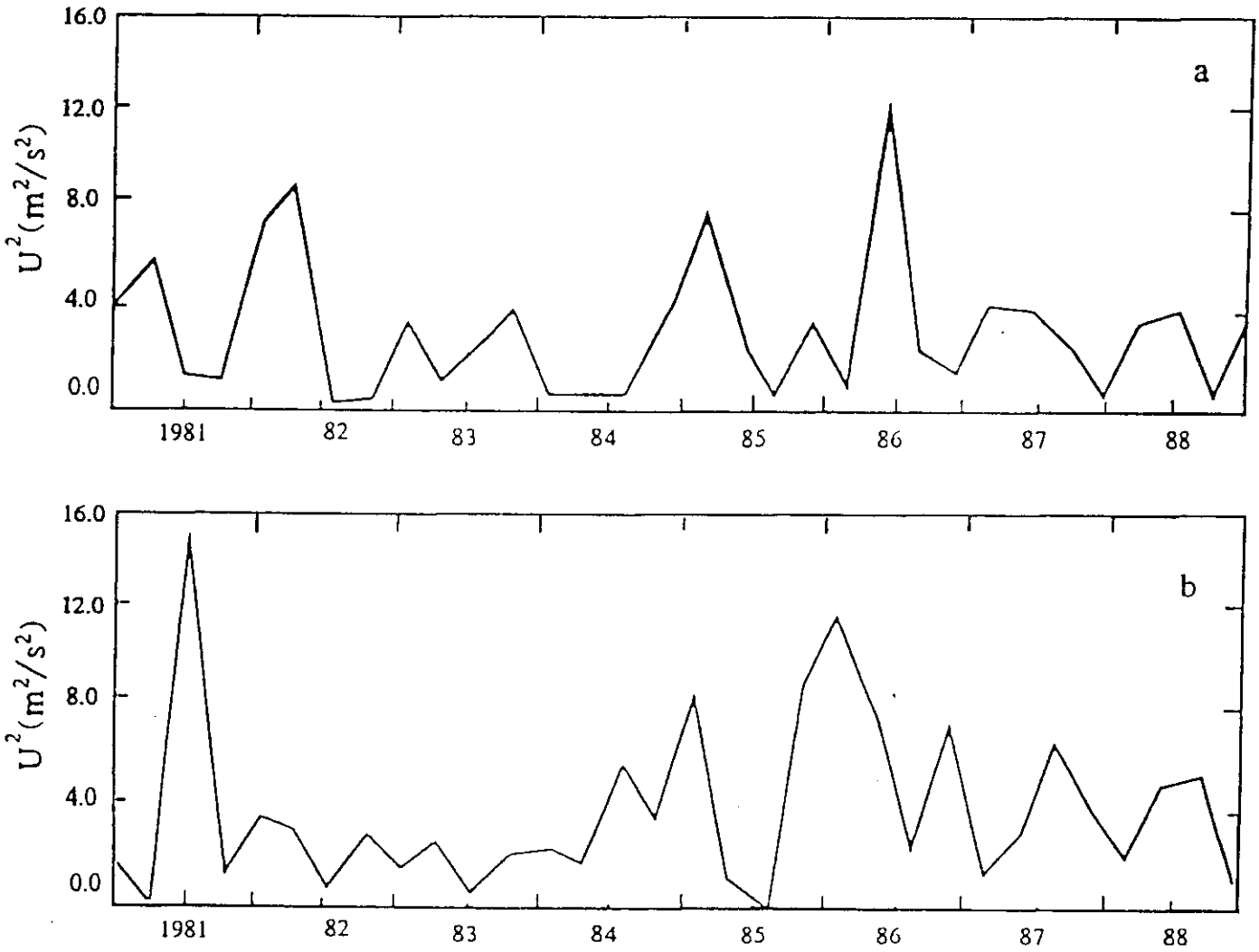

Temporal variations of 30-60 day band-pass filtered u^2 at 200hPa in 10°S-10°N latitudes.a) 160°E-160°W region; b)130°W-11°W region.

Fig.14

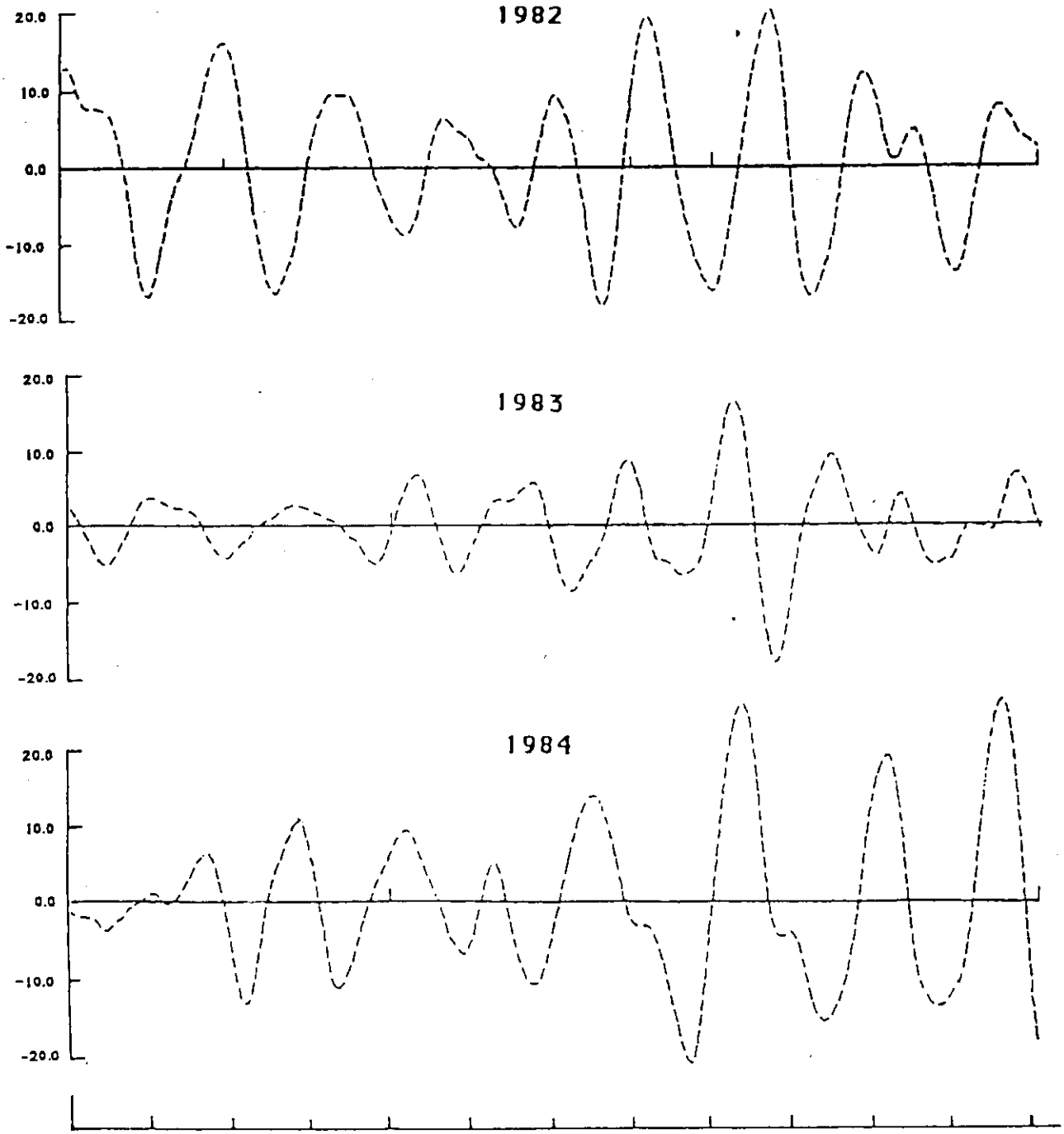

Temporal variations of 30-60 day band-pass filtered OLR (w/m^2) over the equatorial western Pacific in 1982-1983.

Fig.15

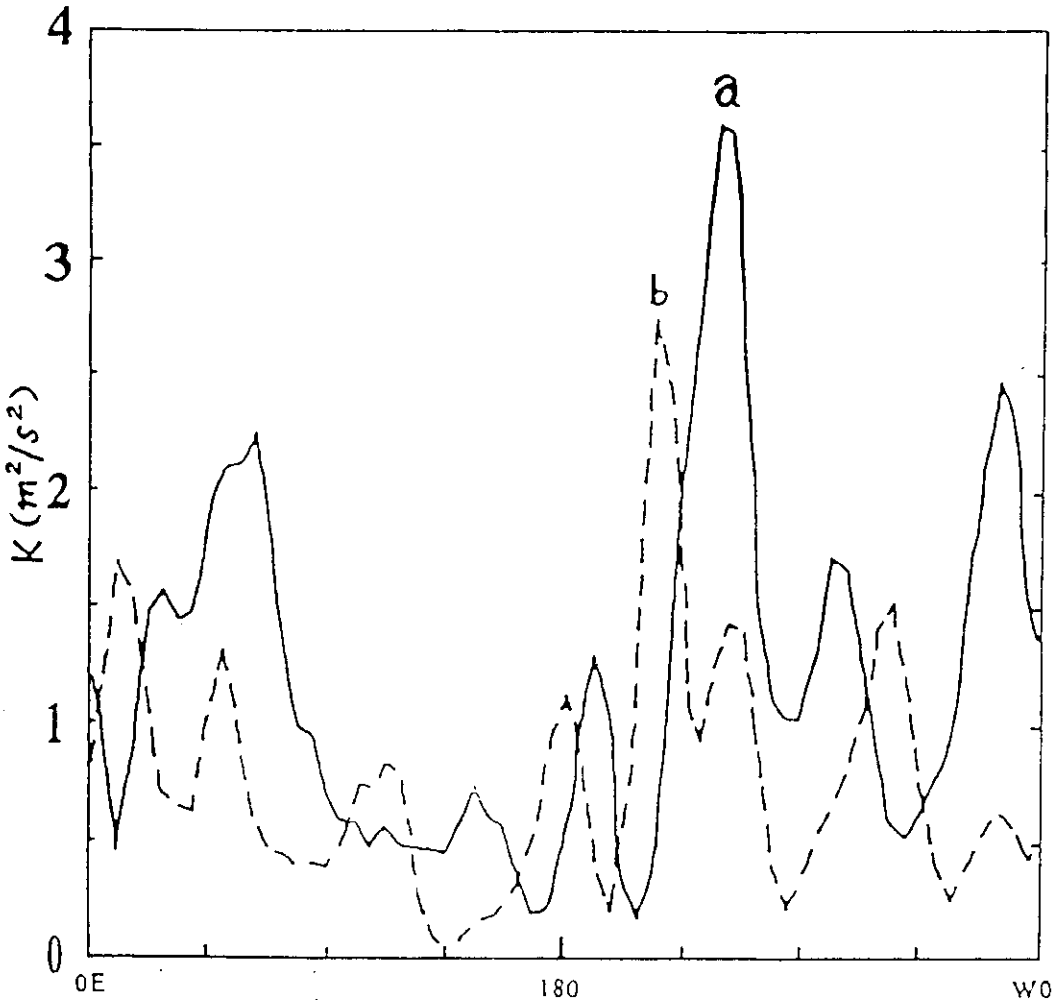

Longitudinal distribution of kinetic energy (K) of the simulated intraseasonal oscillation at 350hPa in 11.1°S-11.1°N latitudes. Solid and dashed line represents the result in the CE and AE, respectively.

Fig.16

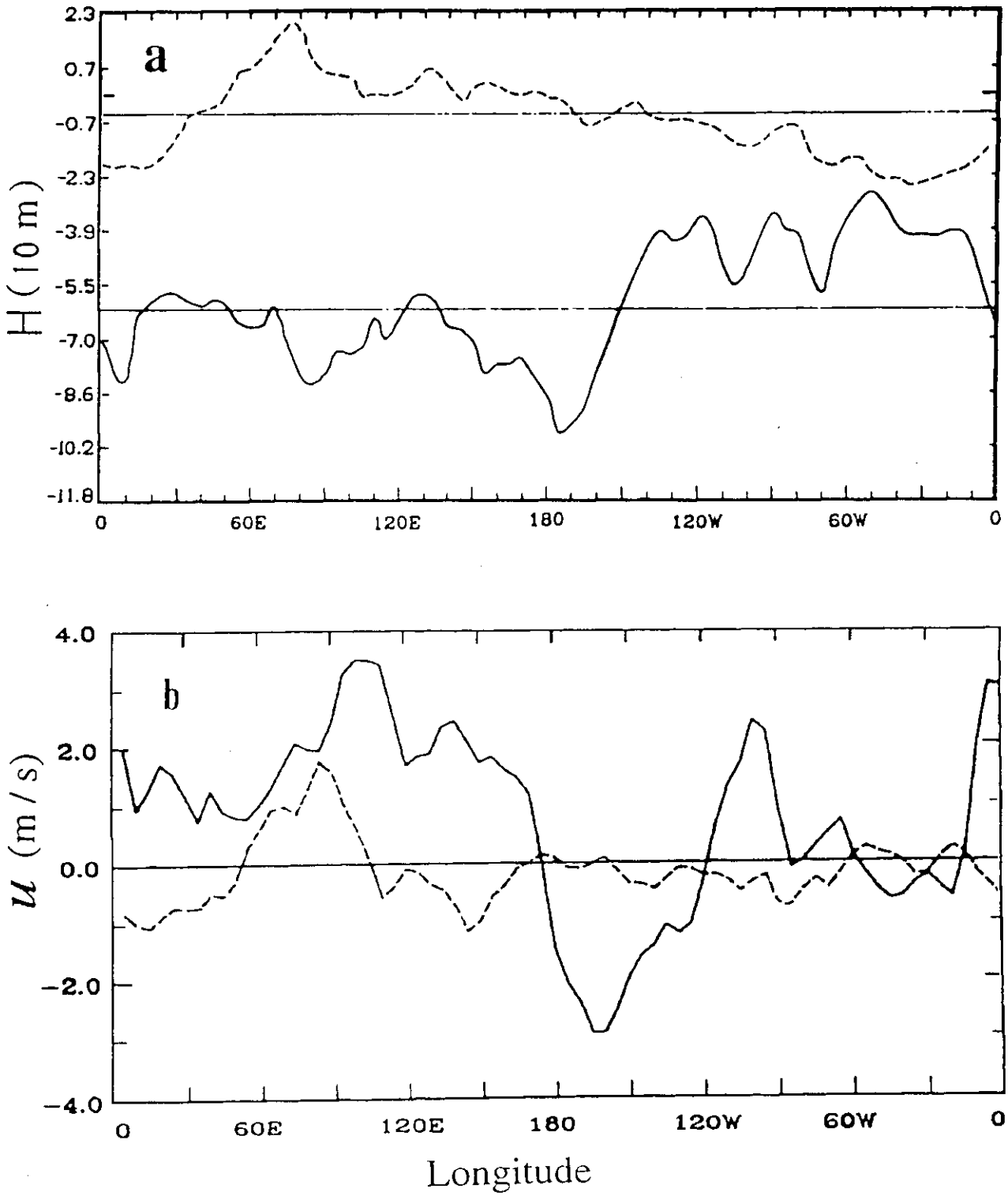

Longitudinal distributions of geopotential height in 1981 summer (a) and zonal wind in 1982 summer (b) for intraseasonal oscillation in the tropics (10°S-10°N). Solid and dashed line respectively represents 200hPa and 850hPa.

Fig.17

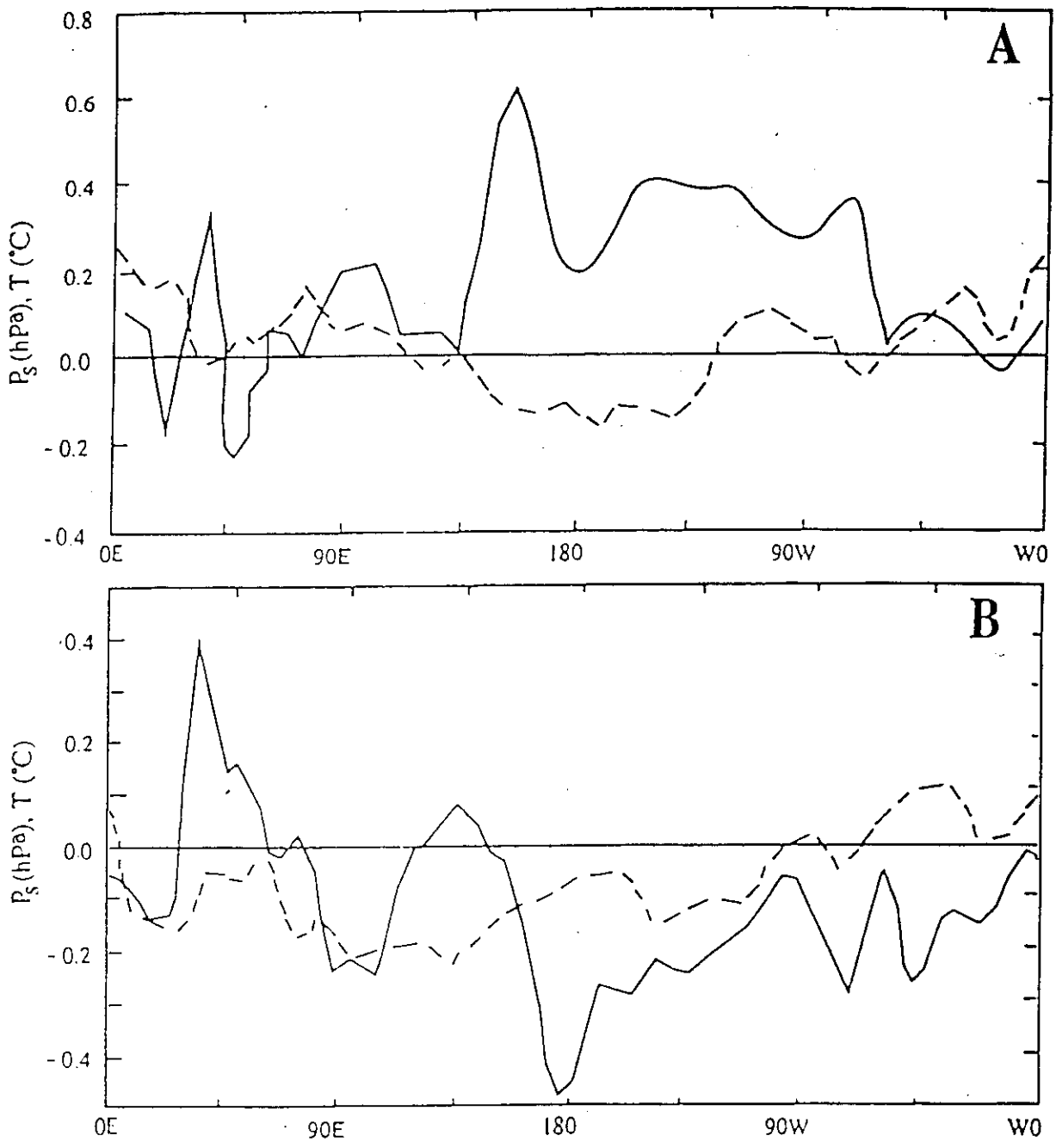

Longitudinal distribution of the surface pressure (solid line) and temperature at 350hPa (dashed line) of the simulated intraseasonal oscillation in the tropics (11.1°S-11.1°N) by using GCM. a) for CE results, b) for AE results.

Fig.18

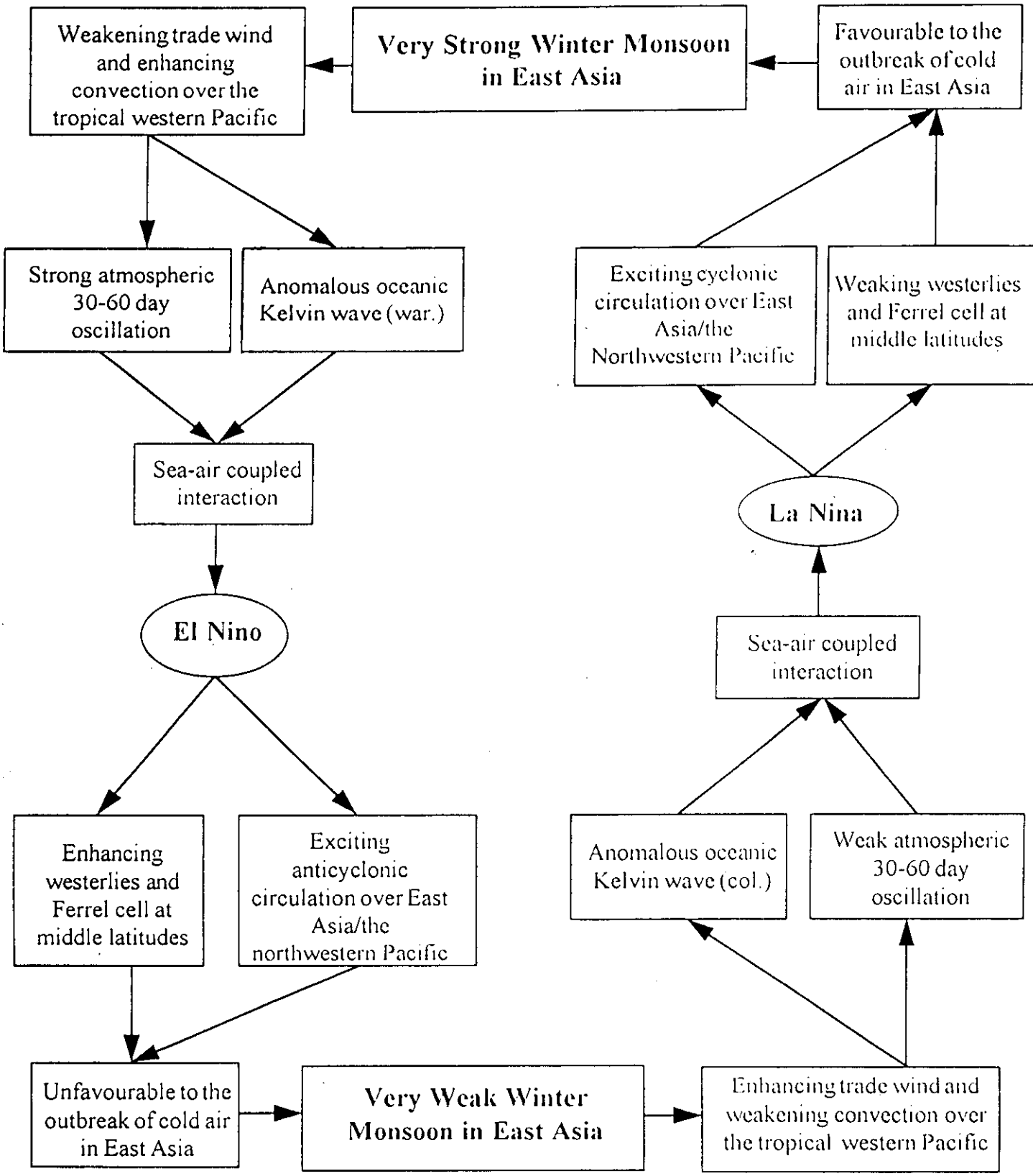

Fig.19 Schematic diagran of the interactions between ENSO cycle and anomalies of winter monsoon in East Asia.

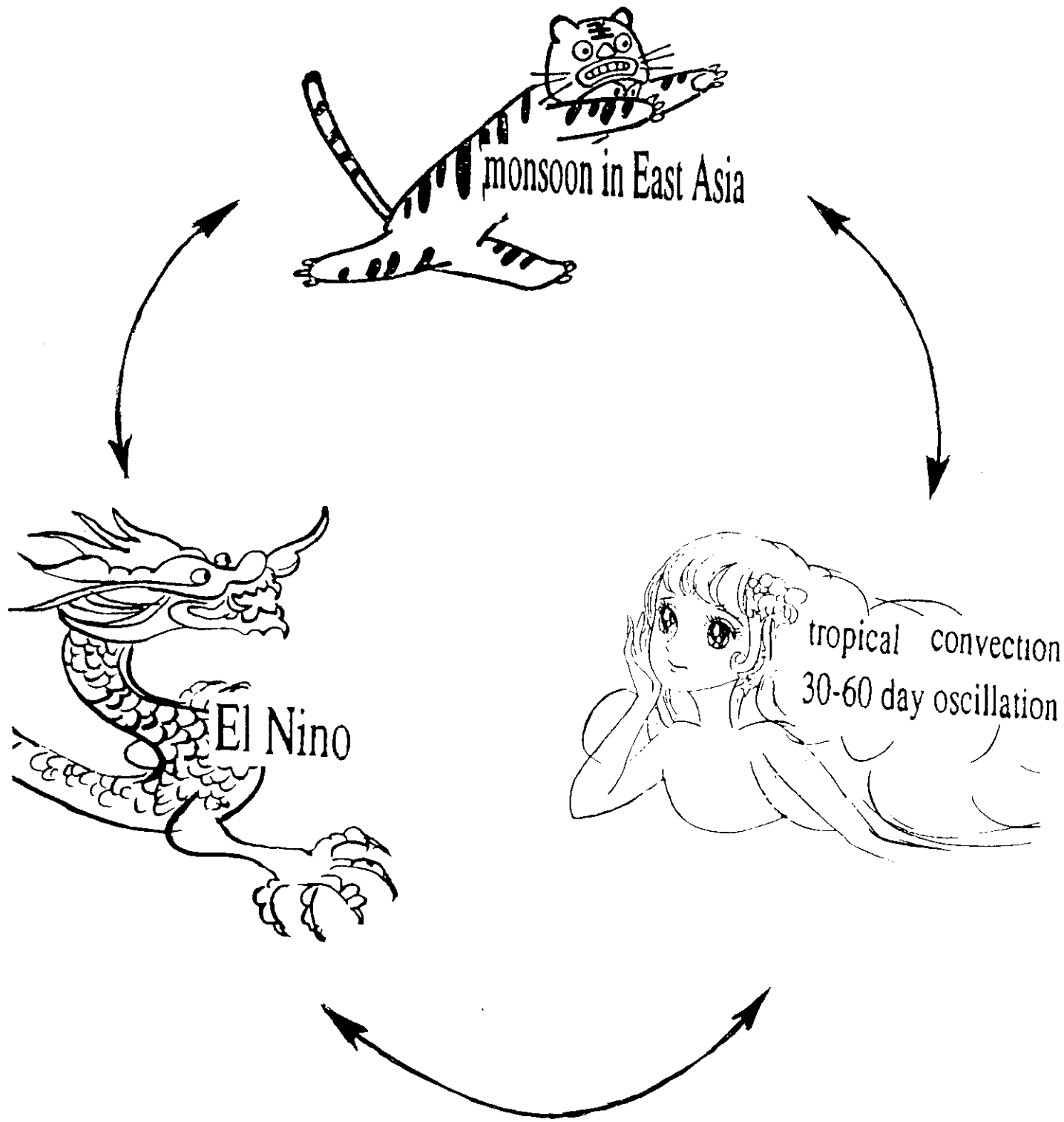

Fig.20 A caricature of the relationship between the monsoon in East Asia, tropical intraseasonal oscillation and El Nino.